A Methodology to Determine Where Septic Systems, Flooded by Sea Level Rise, Impact Shellfish Growing Areas: An Example from Puget Sound, WA

Gabriela Carr

A thesis

submitted in partial fulfillment of the

requirements for the degree of

Master of Marine Affairs

University of Washington

2022

Committee:

Dr. Terrie Klinger

Dr. Sunny Jardine

Program Authorized to Offer Degree:

School of Marine and Environmental Affairs

University of Washington

Abstract

A Methodology to Determine Where Septic Systems,

Flooded by Sea Level Rise,

Impact Shellfish Growing Areas:

An Example from Puget Sound, WA

Gabriela Carr

Chair of the Supervisory Committee:

Dr. Terrie Klinger

School of Marine and Environmental Affairs

Sea levels are projected to rise by as much as 3.3 feet in regions of Washington State by 2100 (Miller et al. 2018). Combined with extreme weather and Washington's already large tidal amplitudes, these projections call into question the fate of low-lying septic systems along Washington's shore. Compromised septic systems on flooded property can leach partially-treated sewage into neighboring shellfish growing areas. Shellfish can concentrate these bacteria and their associated pathogens, making the shellfish dangerous for human consumption. I used information from Kitsap County to determine the risk posed to shellfish growing areas by compromised septic systems under conditions of sea level rise. I identified at-risk septic systems and then used NOAA's GNOME model to determine the likely geographic spread of fecal indicator bacteria following a septic system failure. This methodology was developed with the goal that it can be transferred to other regions of Puget Sound.

Introduction

According to Representative Concentration Pathway (RCP) 8.5 – the highest-emissions scenario predicted by the United Nations Intergovernmental Panel on Climate Change – Washington State will likely (17–83% chance) be subject to 1.4 to 2.8 feet of absolute sea level rise by 2100 (Van Vuuren et al. 2011; Miller et al. 2018). These absolute projections will be modified by local vertical land movement. Coastal regions in Washington are subject to either subsidence or uplift, primarily due to the subduction of the Juan de Fuca plate beneath the North American plate, as well as land decompression in response to glacial retreat 15,000 years ago. On a smaller scale, vertical land movement is also influenced by local faulting and extraction of underground resources (Miller et al. 2018, Appendix C). Tacoma, for example, will likely be subject to 1.9 to 3.3 feet of relative sea level rise under RCP 8.5 by 2100, while under the same scenario, Neah Bay will likely only be subject to 0.3 to 1.7 feet of relative sea level rise (Miller et al. 2018).

Washington's shoreline has extensive low-lying housing and associated infrastructure that will be affected by sea level rise, particularly in the Puget Sound region. In 2019, 77% of the state's population lived in the 12 counties surrounding Puget Sound: Clallam, Island, Jefferson, King (containing Seattle), Kitsap, Mason, Pierce, San Juan, Skagit, Snohomish, Thurston (containing the capitol of Olympia), and Whatcom (US Census Bureau 2019). Twenty-nine percent of the shoreline in these counties is armored, in some form, to protect low-lying infrastructure and housing from current water levels and storm surges (PSP 2021). Sea level rise, in combination with large tidal ranges and increasing storm surge, will increase the risk of flooding of shoreline infrastructure in these counties (Miller et al. 2019).

A key infrastructure concern in the context of sea level rise is coastal on-site septic systems (OSS). When an area is not serviced by a centralized sewer system, wastewater is treated using OSS, either individually for a residence or business or clustered for a small community (US EPA n.d.). They are an important component of sewage treatment in the United States: nation-wide, about 60 million people use OSS at their residence or business, including about 33% of new developments (Hoghooghi et al. 2021, US EPA n.d.).

The design of OSS can vary in complexity and levels of treatment. One of the simplest forms is a gravity system, which includes a septic tank, distribution box, and drain field. Solid waste sinks in the tank, separating from liquid waste. Liquid waste is distributed through drain field lines to surrounding soil, where the waste is consumed by microbes. OSS can include a pre-treatment component, such as a sand filter, which further treats the liquid waste prior to distribution in the drain field. OSS can also have a raised drain field, or a mound, to add space between the liquid waste and the water table below. When microbial or drainage conditions in the soil do not allow the drain field to treat liquid waste successfully, an aerobic treatment unit, combined with a bacterial disinfection unit, can further pre-treat waste prior to the drain field (Seattle & King County Public Health n.d.). OSS have a functional lifespan of approximately 30 to 40 years before needing replacement; however, this depends on their maintenance and use levels (Seattle & King County Public Health n.d.).

Inundation of an OSS drain field, due to flooding or heavy rainfall, can cause waste to leak into nearby waterways, as can poor maintenance of the system. Many of the coastal OSS in Puget Sound are near shellfish growing areas, and once fecal indicator bacteria levels reach a geometric mean of 14 bacteria/ 100 mL water in a growing area, it is no longer safe to use for

harvest (Shehane et al. 2005; Scott Berbells, personal communication). In Puget Sound, shellfish harvest has high cultural and economic value, generating 63% of the ex-vessel value of all the non-Treaty commercial and recreational fisheries (TCW Economics 2008). Nutrients and bacteria from sewage can make shellfish directly and indirectly unsafe for human consumption. For example, shellfish exposed to sewage can accumulate noroviruses, causing gastroenteritis when consumed (Campos & Lees 2014). Runoff can enhance harmful algal blooms by increasing the availability of nitrogen and phosphorus; shellfish concentrate toxins from these algal blooms, making them dangerous to eat (Perri et al. 2015).

Here I combine issues of sea level rise, coastal infrastructure, and the shellfish industry to ask: where will approved Kitsap County growing areas experience high levels of fecal runoff due to OSS flooding as sea levels increase in the coming 50 years? I chose Kitsap County for its extensive, digitized database of its more than 58,000 OSS (Kitsap Public Health District n.d.1). A short ferry ride from the city of Seattle, Kitsap County had a resident population of 271,473 in 2019 (US Census Bureau 2019). Its land is mostly subsiding, exacerbating the impacts of sea level rise (Miller et al. 2018). It currently has 25 approved shellfish growing areas that can be used for commercial shellfish harvest with no threat to public health (WA DOH n.d.1). Harvest sites are primarily owned by the Suquamish and Port Gamble S'Klallam Tribes (Kitsap County 2020). This adds cultural and legal importance to maintaining shellfish harvest opportunities in Kitsap County. According to US v. Washington (1974), the Western Washington Tribes have the right to harvest in their usual and accustomed fishing grounds; in 1994 this decision extended to shellfish, and in 2017 to habitat protection (U.S. v. Washington 1974, 1994, 2017).

The goal of this study is to create a workflow useful for managers in the Puget Sound region, allowing the question of changes in water quality affecting shellfish growing areas to extend beyond Kitsap County. For this reason, I have elaborated on the methodology extensively, including how to obtain the relevant data files, and can provide the accompanying R code upon request: carr.gabriela@gmail.com.

This study uses the General NOAA (National Oceanic and Atmospheric Administration) Oil Modeling Environment (NOAA GNOME) to model where fecal indicator bacteria (FIB) from flooded OSS are likely to reach shellfish growing areas. Designed for managers to simulate oil spills, GNOME treats a spill as a collection of particles. As Engie and Klinger (2007) did in their study of larval dispersal, I am using GNOME particles to represent living organisms, i.e., FIB, rather than oil.

It is important to note that I am assuming that the strong, seaward-flowing surface currents of Puget Sound, created by the difference in density between the bottom waters and the fresher surface waters, are the primary transport mechanism for FIB (Yang and Khangaonkar 2010). I am therefore only using a two-dimensional, surface currents model, although GNOME can be used with a layered approach by adding a Z axis (Zelenke et al. 2012). Because I am not using a Z axis, I have avoided having to parse out density differences between oil, the intended substance represented by GNOME particles, and FIB. Surface waters are also the most relevant to this study because the shellfish growing areas of interest here are in shallow water, close to shore. Lizárraga-Partida and Cárdenas (1996) and Coulliette et al. (2009) have found that FIB are at their highest concentration closest to the shoreline, although Coulliette et al. (2009) note that

the decrease in FIB with distance can be slow if the study area does not become quickly deeper offshore.

GNOME allows users to customize spill simulations further in a wide variety of ways, adding to its utility for managers who want to use my methodology. Users input their own shoreline maps from anywhere in the world, as well as relevant physical factors such as currents and windspeed. Users can then set the location of the spill, as well as the type of oil and time-frame of the spill, and model where the oil flows over time. The particles modeled are Lagrangian elements, followed wherever they flow, and they spread independently and stochastically. To address this stochasticity, GNOME provides the user with a 'minimum regret' trajectory for a spill as well as a 'best guess' trajectory. In this study, I use the minimum regret trajectory. The minimum regret trajectory provides more endpoints for particles than the best guess trajectory, taking into account variations in, for example, wind and current speed; it gives output with 90% certainty (Zelenke et al. 2012).

Methods

I first determined a sample of OSS at high risk by 2070 (a timeframe recommended by WA DOH as relevant to the lifespan of an OSS). I then used the GNOME model (https://response.restoration.noaa.gov/oil-and-chemical-spills/oil-spills/response-tools/gnome.html), combined with Pacific Northwest National Laboratory (PNNL) current solutions of Puget Sound, to model sewage flow over one week. Finally, I found the intersection of this output with approved growing areas of Kitsap County. Figure 1 demonstrates my overall workflow.

I. Datasets

I used datasets from government sources, either provided by state and local agencies or available on the data page of agency websites.

Kitsap County Department of Health provided OSS data for Kitsap County on April 14, 2021. Kitsap County logs its OSS registration data in a living spreadsheet, and therefore the data used here were complete up to that date; real estate parcel owners may have removed or otherwise changed their registration since then. From these data, I extracted three variables: the real estate parcel account identification number (RP_ACCT), the OSS installation date, and the type of OSS.

Real estate parcel data for Kitsap County are available for public access on the county website: https://www.kitsapgov.com/dis/Pages/resources.aspx. I connected OSS to their associated real estate parcels (i.e., those with matching RP_ACCT numbers) using R (version 4.1.3 (2022-03-10) -- "One Push-Up"). This associated each OSS with the geospatial polygon of the real estate parcel. I clipped these polygons to the mean higher-high water by finding the intersection with the boundary line of Kitsap County, removing sections of parcels already underwater. It is important to note that I did not have a precise location for the OSS and drain field within each parcel. This information has not been digitized in Kitsap County, and even in hand-drawn maps is not clear without visiting the site. The number of OSS precluded such visits, as did COVID-19 concerns.

Geospatial data for shellfish growing areas for Washington State are available for public download: https://doh.wa.gov/data-statistical-reports/data-systems/geographic-information-system/downloadable-data-sets. These show the boundaries of growing areas that are approved as

well as those that are not currently approved for use. I selected only the boundaries of growing areas currently approved for use.

To provide clarity for the reader, I have included a boundary of Kitsap County as well as Washington State in maps provided here. A boundary line of Kitsap County, reaching to the mean higher high-water level, is available for public download on the same page as parcel data: https://www.kitsapgov.com/dis/Pages/resources.aspx. A coarse outline of Washington State is available for public use through the United States Census Bureau: https://www.census.gov/geographies/mapping-files/time-series/geo/carto-boundary-file.html. A fine-scale map of the Pacific Northwest, better showing the many details of Puget Sound inlets, passages, and islands, is available publicly from the data catalog of the United States Geological Survey, specifically from their 2006 "Seaside, Oregon, Tsunami Pilot Study": https://pubs.usgs.gov/ds/2006/236/catalog.shtml#GIS_data_table.

Miller et al. (2018) have provided open access geospatial data for their Washington State sea level rise projections: https://wacoastalnetwork.com/research-and-tools/slr-resources/. These projections incorporate elevation, but the geospatial data do not, instead dividing Washington State into rectangles associated with a particular mean sea level rise over time. The data provided are for relative sea level rise, not absolute sea level rise. They therefore take into account tectonic activity in the Puget Sound area, including both uplift and subsidence (Miller et al. 2018).

NOAA's sea level rise viewer includes downloadable inundation layers for up to 10 feet of sea level rise for all states and territories: https://coast.noaa.gov/slrdata/. These geospatial layers incorporate elevation and are available in 1-foot increments.

T. Khangaonkar (PNNL) provided solutions of the Salish Sea Model for use in the NOAA-GNOME program. These solutions, compiled at an intermediate resolution, include daily Puget Sound currents for all of 2014.

To determine the 7-day periods with the heaviest and lightest precipitation of 2014, I obtained daily rain data for that year from the Kitsap Public Utility District, available online: http://kpudhydrodata.kpud.org/APSFED_RAIN.aspx.

II. Determining Septic Risk

I determined the risk of discharge associated with each shoreline parcel by adding three factors: (1) the percent inundation of the associated parcel, based on the flooding scenario elaborated below, (2) the type of OSS, and (3) the age of the OSS. A parcel was determined to be a shoreline parcel if it had any intersection with 1.5 feet of sea level rise.

Because I did not have precise locations for each OSS and its drain field, I used the percent inundation of the parcel under 4 feet of flooding (including both sea level rise and extreme weather) to approximate the likelihood of inundation. I chose 4 feet based on the sea level rise and extreme weather projections of Miller et al. (2018, 2019) for Kitsap County. According to this simulation, under RCP 8.5 there is a 17% chance that the average sea level rise in Kitsap County will be 1.64 feet by 2070, with the median sea level rise 2.20 feet; there is a 50% chance that the average sea level rise will be 1.237 feet, with a median of 1.600 feet. IPCC categorizes 17–83% chance of occurrence to be "likely," with Raymond et al. (2020) recommending choosing a lower likelihood scenario for high-impact infrastructure, such as septic tanks. I therefore chose 1.5 feet of sea level rise, an intermediate level between the 17% and 50% predictions that includes a corresponding prediction for extreme water level. Miller et al. (2019) modeled 3.7, 4.1, and 4.4 feet of flooding

from 2-, 5-, and 20-year floods, respectively, with 1.5 feet of sea level rise. To account for elevation when estimating the percent inundation of parcels, I used NOAA sea level rise inundation layers; these are only available in full foot increments. Using R, I found the intersection of the 4-foot inundation layer and the septic-parcel data. I used this percent inundation as an estimate of likelihood of inundation of each parcel's drain field.

I determined the risk level (Table 1) of each type of OSS by referring to Miller et al. (2017) and consulting with both the Washington Department of Health and the Kitsap Public Health District. Miller and Mastriani (2017) assigned the risk level of different types of OSS on a scale from 1 to 6; their classification included many of the types of OSS used in Kitsap County. I consulted with the Washington Department of Health and Kitsap Public Health District, who were able to provide information on the systems not covered by Miller and Mastriani (2017) and to adjust the scale based on their local expertise.

I assigned risk level based on the assumption that the systems will not be submerged under conditions of 1.5 feet of sea level rise, but that they will experience intermittent flooding due to storm surge, which adds about 2.5 feet of further inundation (Miller et al. 2019). I assigned Large Onsite Sewage Systems (LOSS) a score of 1, the minimum risk. Because these systems handle 3,500 to 100,000 gallons a day, they are monitored closely by the Washington Department of Health and restricted in their proximity to bodies of water (WA DOH n.d.2). They are also required to have renewed operating permits annually. Small-scale OSS in Kitsap County require inspections once every 1 or 3 years, depending on the type (Kitsap Public Health District n.d.2).

The remaining types of OSS are either of an unknown type, which I assigned the highest risk, or fall under four different treatment level types, according to the Washington Department of

Health. The higher the level of pre-treatment that a system performs prior to release into the drain field, the lower the assigned risk level; these systems are allowed in locations with a high water table or closer to the shoreline (Kitsap Public Health District n.d.2). No systems of the pre-treatment level type D were present among shoreline OSS in Kitsap County, and there is therefore no risk level 4 represented in the data. In assigning risk levels I assumed, based on the advice of R. Parker (WA DOH), that (a) no system was given a waiver to be closer to the water table than normally permitted for that system and (b) all systems are maintained in working order. It should be noted that commercial or residential status was not included in this dataset.

I determined OSS age by calculating the time from date of installation to the present in years. The OSS dataset does not include maintenance status of each OSS; I therefore used age as a proxy for the condition of the OSS.

To determine the overall risk for each OSS, I added its percent inundation (on a scale from 0 to 1), type (rescaled from 0 to 1) and age (rescaled from 0 to 1), following the example of Miller and Mastriani (2017); I then rescaled the sum from 0 to 1. Plotting the total risk of each OSS as a histogram (Figure 2), there was a noticeable break between the highest risk OSS (total risk >0.95) and the others. I selected all OSS with risk levels above 0.95, creating a pool of 1647 shoreline OSS at highest risk. From this pool, I took a single random sample of 100 OSS, setting a seed for reproducibility (Figure 3). By taking a single random sample across this high risk pool, rather than first stratifying by OSS type and/or taking multiple random samples, it is possible that I have over- or under-represented particular types or locations of OSS.

III. Determining Growing Area Vulnerability – GNOME Simulation

The PNNL deterministic current solutions for GNOME available for this study were created at a lower resolution than the OSS/ parcel data, and GNOME cannot run simulations where the spill begins on land; consequently, I used the closest approximation on the shore as spill starting points. After determining the centroid point for each of the highest risk parcels sampled, I attempted to run GNOME using that centroid. If that centroid point was on land, I used Google Maps, in conjunction with GNOME, to manually find the closest point for a spill starting point in the model. If possible, I chose spill starting points that were perpendicular to the shoreline edge of the parcel. If the parcel was in an inlet that was not shown in GNOME, I chose the closest available point. With these adjustments, spill starting points were, on average, 326.04 meters from the centroid of the relevant parcel (median: 242.73 meters; maximum: 2,341.12 meters; minimum: 0.04 meters).

I simulated spills from the 100 starting points for two 168-hour (7-day) time periods: March 2 – March 9, 2014 (1:00 AM to 1:00 AM) and September 3 – September 10, 2014 (1:00 AM to 1:00 AM). These corresponded with periods of minimum and maximum rainfall in 2014, respectively. Seasons with higher rainfall, associated with flooding and sediment erosion, correlate with higher fecal indicator bacteria (FIB) in coastal waters than do seasons with lower rainfall (Couliette et al. 2009; Lipp et al. 2001). Each spill consisted of 1,000 particles representing FIB, simulating a 360-gallon spill over the first 24 hours. A volume of 360 gallons is used by WA DOH to approximate the mean daily flow for an OSS, assuming an average household of 3 bedrooms and 2 people per bedroom. I used 1,000 particles per spill because that is the minimum number of particles that GNOME can release in the minimum regret solution mode while maintaining

statistical significance. I used 24-hour release periods based on Yang et al. (2019) Puget Sound storm surge simulations, which were 24 hours in length; storm surge can be longer or shorter than this time frame. This storm surge accounted for the 2.5 feet of the 4 feet of flooding that was not due to sea level rise, but instead to extreme weather.

I used settings for the model primarily based on an example provided by T. Khangaonkar (PNNL) and following Engie and Klinger (2007). Along- and cross-current uncertainties were set at 1%, with velocities set at 1 inch equal to 10 meters/second and a multiplicative scalar of 1. I set refloat half-life for each particle at 168 hours, i.e., the entirety of the simulation, assuming that particles would not refloat once beached. I made this assumption because (a) FIB can remain in intertidal growing areas, and in shellfish themselves, for multiple days and (b) FIB attach to sediment (Martínez et al. 2009; Lipp et al. 2001). I ran spills with the default computational time step of 0.25 hours, matching the methodology of Engie and Klinger (2007). I ran all 100 trials simultaneously using the "minimum regret solution": this output provided the 90% likelihood spill scenario, precluding the need to run multiple simulations and take an average. I did not allow particles to "land jump," preventing GNOME from using a simplified algorithm that ignores the path of the particle.

Results of the GNOME simulation were output as KML files for the "current model time" (March 2 – March 9 or September 3 – September 10, 2014), with output for every 24-hour interval. Because I had turned off the refloat option, this longer interval did not miss any particle movement; it also allowed me to model a full week without running into limitations of computing power and run time. Finally, I mapped the particle distribution for each approved shellfish growing area in Kitsap County (Figures 4 and 5).

Results

I binned particle distribution results into hexagonal cells to visualize the entire growing area at once while identifying regions where particles consistently landed. I have included visualizations of only those growing areas that accumulated 1000 or more particles over the course of each 7-day period. Twenty of the 25 Kitsap County growing areas currently approved for use by WA DOH met my criteria for visualization (Figure 4). After 7 days, 99% of the particles had beached in both simulations, with 28.49% of particles in growing areas for the March simulation and 29.01% for the September simulation.

Bainbridge Island South

The Bainbridge South growing area accumulated 8,039 and 8,215 particles in the March (Figure 6) and September (Figure 7) simulations, respectively. Three of the spills started within or adjacent to the western side of the growing area. From 24 hours after the spill started and on, both simulations maintained the highest concentrations of particles on the western side. Two of the hexagonal cells accumulated the highest number of particles, with about 400 to 600 particles each. Particles spread across the growing area more quickly in the drier September simulation, dispersing across the growing area by the 24-hour mark. For the rainier March simulation, particles remained on the western side of the growing area for the first 24 hours, dispersing to the rest of the growing area by the second day.

Port Blakely A

The Port Blakely A growing area accumulated 5,616 and 6,410 particles in the March (Figure 8) and September (Figure 9) simulations, respectively. One spill started within the southwestern end of the growing area. From 24 hours after the spill started and on, both simulations

maintained the highest concentrations of particles on the southwestern side. One of the hexagonal cells accumulated the highest number of particles, about 300 particles, with relatively high accumulations in the cells around it. For both simulations, particles were spread offshore in the growing area at the 24-hour mark, but were almost all beached by the 48-hour mark.

Port Blakely B

The Port Blakely B growing area accumulated 31,451 and 33,521 particles in the March (Figure 10) and September (Figure 11) simulations, respectively. Six spills started within or adjacent to the western side of the growing area. From 24 hours after the spill started and on, both simulations maintained the highest concentrations of particles on the western side. Five adjacent hexagonal cells accumulated the highest number of particles, between 600 and 1000 each. These cells are located close to the spill sites. For both simulations, particles were spread offshore in the growing area at the 24-hour mark but were almost all beached by the 48-hour mark. 96 hours after the spill began, some of the particles were spread far offshore in the September simulation, suggesting an influx of particles from outside of the growing area.

Colvos Passage

The Colvos Passage growing area accumulated 4,545 and 4,536 particles in the March (Figure 12) and September (Figure 13) simulations, respectively. One spill started within the southwestern side of the growing area, and the area around this spill had the highest accumulation of particles throughout the week. The two cells closest to the spill site had the highest concentration for both simulations, ranging from about 250 to over 400 particles. The distribution of particles remained consistent throughout both simulations, with particles mostly beached in both by the 24-hour mark. Colvos Passage is a particularly narrow growing area, close to shore, so by filtering for

particles in this growing area I output primarily those that were beached. Particles spread more evenly across the north end in the March simulation and were more clustered in the September simulation.

Dyes Inlet

The Dyes Inlet growing area accumulated 1,399 and 1,590 particles in the March (Figure 14) and September (Figure 15) simulations, respectively. One spill started within the northwestern corner of the growing area, but in this case it was the western and southeastern sides of the growing area that had the highest accumulation of particles during the week. In the March simulation, a single hexagonal cell had the highest accumulation, reaching about 60 particles by the 144-hour mark. In the September simulation, both sides of the growing area showed more equal levels of accumulation. In both simulations, particles were dispersed across the water most broadly at the 24-hour mark and had mostly beached by the 48-hour mark.

Foulweather Bluff East

Foulweather Bluff East growing area accumulated 6,681 and 6,758 particles for the March (Figure 16) and September (Figure 17) simulations, respectively. One spill started adjacent to the southwest corner of the growing area, and the hexagonal cell with the highest accumulation throughout the week, in both simulations, was next to this spill. This cell accumulated between 400 and 500 particles throughout the week. The two cells around it showed much lower accumulations with almost no particles beyond, suggesting that most of the spill adjacent to the growing area beached there immediately.

Port Gamble

The Port Gamble growing area accumulated 6,997 and 7,109 particles in the March (Figure 18) and September (Figure 19) simulations, respectively. One spill started adjacent to the southeast corner of the growing area, and the cell with the highest accumulation for both simulations was in the area next to this spill. In both simulations, this cell accumulated more than 600 particles throughout the week. The two cells on either side had much lower accumulations of about 100 particles, with the remaining particles beached at low concentrations throughout the growing area.

Hood Canal #1B

The Hood Canal #1B growing area accumulated 5,844 and 6,041 particles in the March (Figure 20) and September (Figure 21) simulations, respectively. One spill started adjacent to the northeast corner of the growing area, and the hexagonal cells with the highest accumulation of particles for both simulations were in the area next to this spill. In both simulations, a single cell with between 600 and 800 particles remained there during the week, although the location of the cell shifted slightly south for some time stamps. Remaining particles beached at lower accumulations first primarily in the northeast corner of the growing area, then spreading south until they had beached. Particles in the March simulation spread farther south than in the September simulation, reaching the boundaries of the growing area.

Hood Canal #2C

The Hood Canal #2C growing area accumulated 18,664 and 18,858 particles in the March (Figure 22) and September (Figure 23) simulations, respectively. Four spills started adjacent to the south side of the growing area, with the four clustered into two pairs. The two cells next to the central pair of spills accumulated about 1000 particles each in both simulations throughout the

week, while the grid cell closest to the southern pair of spills accumulated only about 300 particles. The remainder of the particles beached almost completely by the 24-hour mark in both simulations, spread relatively consistently throughout the growing area.

Hood Canal #4

The Hood Canal #4 growing area accumulated 6,030 and 4,660 particles for the March (Figure 24) and September (Figure 25) simulations, respectively. Two spills started adjacent to the northeast corner of the growing area, and the cell with the highest accumulation of particles in both simulations was next to one of these spills. In the March simulation this grid cell accumulated about 800 particles, while in the September simulation it accumulated about 500 particles. This grid cell maintained the highest accumulation throughout the week, with remaining particles spread much more sparsely. All particles stayed in the northeast quadrant of the growing area in the March simulation, while particles spread south from the 48-hour mark on in the September simulation.

Kingston A

The Kingston A growing area accumulated 6,433 and 6,555 particles in the March (Figure 26) and September (Figure 27) simulations, respectively. One spill started adjacent to the center of the growing area, and the single cell with the highest accumulation of particles in both simulations was next to this spill. In the March simulation this grid cell accumulated about 800 particles, while in the September simulation it accumulated about 700 particles, with slightly fewer particles by the end of the week. This grid cell maintained the highest accumulation throughout the week, with remaining particles spread much more sparsely in the growing area. Most particles beached throughout the growing area by the 48-hour mark.

Kingston B

The Kingston B growing area accumulated 5,573 and 6,963 particles in the March (Figure 28) and September (Figure 29) simulations, respectively. One spill started adjacent to the center of the growing area, and the single cell with the highest accumulation of particles for both simulations was next to this spill. In the March simulation this grid cell accumulated about 500 particles, with slightly fewer particles by the end of the week, while in the September simulation it accumulated about 750 particles. This grid cell maintained the highest accumulation throughout the week, with remaining particles spread much more sparsely in the growing area. Most particles beached throughout the growing area by the 48-hour mark for the September simulation and the 72-hour mark for the March simulation.

Liberty Bay

The Liberty Bay growing area accumulated 8,306 and 7,565 particles in the March (Figure 30) and September (Figure 31) simulations, respectively. One spill started adjacent to the center of the growing area, and the three cells with the highest accumulation of particles in both simulations were near this spill. In both simulations, the cell with the highest accumulation had about 350 particles. The cell adjacent to the east had the second highest accumulation, and the two cells directly above had the third, in both simulations. The remaining particles beached sparsely along the growing area by the 24-hour mark. This growing area demonstrates the difference in resolution between the Kitsap County boundary in the GNOME simulation and the one I used in geospatial analysis and mapping. Particles appear to beach offshore in this growing area because they beached in the GNOME simulation, which uses a map of Kitsap County's shoreline that is less precise than the Kitsap County boundary I used in other parts of this methodology.

Port Madison

The Port Madison growing area accumulated 35,550 and 36,507 particles in the March (Figure 32) and September (Figure 33) simulations, respectively. Fourteen spills started within or adjacent to the growing area, primarily in the northern half. The cell with the highest accumulation of particles in both simulations was in the center of the northern side of the growing area, adjacent to a cluster of two spills. In both simulations this grid cell accumulated approximately 1600 particles, with a slight decrease in accumulation by the end of the week. The remainder of the particles were concentrated more heavily in the northern half of the growing area; most particles had beached by the 24-hour mark.

Miller Bay

The Miller Bay growing area accumulated 1,398 and 1,149 particles in the March (Figure 34) and September (Figure 35) simulations, respectively. No spills started within or adjacent to the growing area. Particles were spread relatively consistently throughout the growing area, with a slight concentration on the eastern side. The grid cells with the highest accumulations contained only about 22 particles.

Port Orchard A

The Port Orchard A growing area accumulated 18,111 and 18,080 particles in the March (Figure 36) and September (Figure 37) simulations, respectively. Three spills started within or adjacent to the growing area, two in the northern half and one in the southeastern corner. The cell with the highest accumulation of particles in both simulations was adjacent to one of these spills, containing about 900 particles, with a slight decrease in accumulation by the end of the week. The two cells with the second highest concentration were adjacent to the other two spills and contained

about 500 to 600 particles. The remainder of the particles were spread out through the water at the 24-hour mark, but mostly had beached by the 48-hour mark.

Port Orchard B

The Port Orchard B growing area accumulated 14,658 and 14,220 particles in the March (Figure 38) and September (Figure 39) simulations, respectively. Five spills started within or adjacent to the growing area, with four in the southwest corner. The cell with the highest accumulation of particles for both simulations was adjacent to the northern-most spill and contained about 600 particles. The cells with the second highest concentration were in the southwest corner and contained about 200 to 300 particles each. The remainder of the particles had beached along the length of the growing area by the 24-hour mark. It is interesting to note that the single northern-most spill resulted in a higher concentration of adjacent particles by the 24-hour mark than the cluster of four spills on the southwest corner, suggesting that the coastline of that upper inlet allows more particles to beach.

Port Orchard C

The Port Orchard C growing area accumulated 2,919 and 1,415 particles for the March (Figure 40) and September (Figure 41) simulations, respectively. One spill started adjacent to the growing area. The single cell with the highest accumulation of particles for both simulations was on the southern end of the growing area, closest to a spill that was nearby, but not adjacent to the growing area and therefore off the map. Accumulation in this cell increased over the week in the March simulation, reaching over 200 particles. In the September simulation, which accumulated noticeably fewer particles than the March simulation, this cell only accumulated about 75 particles. For this simulation, the cell adjacent to the northern spill accumulated a similar number of particles

as the peak cell. As time went on, this second cell near the northern spill accumulated more particles. The remainder of the particles beached sparsely along the length of the growing area by the 24-hour mark.

Yukon Harbor

The Yukon Harbor growing area accumulated 9,035 and 10,739 particles in the March (Figure 42) and September (Figure 43) simulations, respectively. Three spills started adjacent to the growing area in the northwest corner of the growing area. The single cell with the highest accumulation of particles was adjacent to one of these spills and contained about 600 particles in each simulation, although this fluctuated throughout the week. The cell with the second highest accumulation (at some points binned with its neighbor as one cell) was adjacent to the other two spills and contained about 450 particles. The remainder of the particles primarily stayed in the northwest corner of the growing area. In the September simulation, particles also spread sparsely south throughout the rest of the growing area, while particles remained almost exclusively in the northwest corner of the March simulation.

Discussion

My analysis demonstrates the potential for spatial differences in the spread of fecal bacteria and emphasizes that growing areas adjacent to risky OSS will likely accumulate the highest concentrations of FIB. Many growing areas showed a strong concentration of FIB close to a failing OSS while the remainder of FIB in the growing area were spread more sparsely. This is largely a result of my choice to prevent FIB from refloating. According to my parameters, once particles are beached in a growing area, they remain beached, resulting in high concentrations adjacent to a spill. The assumption that FIB do not refloat once beached is reasonable, given their affinity to

adhere to substrates. It also suggests that, if a user of this methodology wishes to continue to keep the refloat option functionally off, then they do not necessarily need to use GNOME to understand where adjacent, failing OSS will most impact growing areas.

Although others have shown that rainfall can be correlated with higher FIB levels in waterways near wastewater infrastructure, the simulations indicate that growing areas mostly accumulated similar numbers of particles regardless of season. Two notable exceptions are Hood Canal #1A and Port Orchard Passage C, which had 209% and 206% more particles in the rainy March simulation than the dry September one. Neither growing area appears to be at the mouth of a waterway in the GNOME simulation, which would have explained this disparity through increased inflow of contaminated freshwater. These two growing areas therefore could merit particular attention when monitoring after storms, as it is possible that increased rainfall carries contaminated freshwater along the coast here from a waterway that is not adjacent to them.

While FIB can come from agricultural and stormwater runoff, malfunctioning OSS have been repeatedly identified as important, and often overlooked, FIB sources (e.g., Chinnadurai et al. 2020; Cahoon et al. 2006). This is further complicated by varying levels of oversight of OSS, which are often monitored only by homeowners themselves, and sometimes not at all. Coastal homeowners may not be aware, for example, that their OSS may need repairs after flooding, and even if they are, such repairs can be prohibitively expensive (Simmons et al. 2018; Cox et al. 2020). Kitsap County is addressing this financial burden in collaboration with Craft3, which provides loans for OSS repair or replacement; loan rates are scaled based on income and do not require excellent credit scores (Craft3 n.d.). Nevertheless, ultimately homeowners are responsible

for the entire cost through loan payments, suggesting the possibility that some may avoid these repairs to avoid the prohibitive cost.

As sea levels rise and storm surge increases in the coming decades due to climate change, the FIB contribution from OSS will likely increase in coastal communities. OSS drain fields require oxygen and consistent drainage of soil for microbes to breakdown effluent successfully. Rising sea levels, impacting both groundwater level and mean height of high water, combined with storm surge will increasingly inundate shoreline drain fields (Cooper et al. 2016). Although this study has focused on sea level rise, and primarily on surge over a drain field rather than inundation from rising groundwater, temperature increases due to climate change can also impact OSS functionality. For example, increased temperature will decrease the amount of oxygen available to microbes in drain field soils (Cooper et al. 2016). Older OSS with lower levels of pre-treatment, prior to release into the drain field, will likely leak more FIB when inundated. Because shellfish growing areas are closed when the geometric mean bacterial count is greater than 14 FIB/ 100 mL, they are particularly sensitive to any increase in FIB under changing climate conditions (Scott Berbells, personal communication; Cahoon et al. 2006).

One solution that some communities are pursuing, where residences and businesses are sufficiently dense, is to convert from OSS to centralized wastewater systems (Allen et al. 2019). Parts of Kitsap County are moving from OSS to sewer systems in the coming years (WA DOH, personal communication). It is important to note that while centralized wastewater systems can be more closely monitored and controlled than OSS, they can nevertheless also be sources of FIB, particularly when overwhelmed during heavy rain, resulting in discharge of excess wastewater (King County Department of Natural Resources and Parks 2020). They are also often constructed

at low elevations along the coastline to allow most of the incoming sewage to flow to the treatment facility by gravity, instead of by pumping. This can make these facilities vulnerable to flooding by rising groundwater and storm surge (Hummel et al. 2018). The methods I used here focus narrowly on problematic OSS; it could therefore be useful to update this model as parts of Kitsap County move to a centralized system, removing any OSS that have been taken out of commission.

A limitation of using the GNOME model is that it is not designed for living particles, and therefore does not model the changing amount of FIB as they rise and fall after a spill. I chose non-weathering particles as the best analog, as FIB do not decay in the same trajectory as GNOME models oil degradation. On the contrary, in some cases FIB may even multiply outside of mammalian gastrointestinal systems if nutrients are available (Bolster et al. 2005).

Physical conditions in Puget Sound around Kitsap County are likely to increase persistence of FIB, further confirming the choice to use non-weathering particles. Testing at points on the west and east sides of Kitsap County (Hood Canal and Sinclair Inlet, respectively) from 1993 to 2002 found the monthly mean temperature to range from 8 to 14 degrees Celsius at the surface. For the same period, salinity ranged monthly from 28‰ to 30‰ (Moore et al. 2008). Higher salinity can increase persistence of FIB, possibly by reducing predation on the bacteria, although notably this varies by FIB species (Schulz and Childers 2011; Anderson et al. 2005). Higher temperatures, conversely, increase inactivation rates, exacerbating the negative impacts of solar irradiation on bacteria (Sinton et al. 2007). Schulz and Childers (2011) found that the combination of 10°C and 30‰ salinity, comparable to average conditions in Kitsap County, resulted in the lowest decay rates among the three temperatures (10, 20, and 30°C) and 3 salinities (0, 5, and 30‰ salinity) tested.

The analytical technique that I used does not explicitly account for windspeed, although GNOME does have the capacity to incorporate wind data. A model of an emergency bypass outfall from King County's West Point Treatment Plant, located just east of Kitsap County across Puget Sound, provides a useful comparison. That draft report found that while wind had no impact on the speed of FIB reaching some growing areas in Kitsap and King Counties, in other growing areas increased wind speeds could decrease arrival times from about 21 hours to about 4 mins (King County Department of Natural Resources and Parks 2020). Wind is therefore likely to play a factor in the speed with which bacteria reach certain growing areas.

A notable challenge in the use of this analytical technique is determining spill starting points that will run in GNOME. This situation can be improved by obtaining a higher resolution currents solution for Puget Sound; however, the feasibility of this approach depends on funding availability for the project. A second solution could be to obtain a geospatial data file of the landmass at the intermediate resolution of the GNOME model. The closest point to each OSS centroid on the perimeter of that landmass can then be determined using R.

For future applications, this technique will benefit by taking at least two additional OSS variables into account: (1) the status of the OSS as commercial or residential and (2) the septic tank capacity per bedroom. A commercial system has a higher inherent risk than a residential system because it manages a larger quantity of sewage (Roger Parker, personal communication). Similarly, the more bedrooms in a residence, the higher the sewage flow. Hoghooghi et al. (2021) found that, when assessing OSS vulnerability to rising groundwater, septic tank capacity per bedroom was the second most important predictor variable regarding vulnerability, after drain field type.

A second improvement would be to incorporate results into an interactive Leaflet visualization (Gaul 2016). Currently, the pilot addHexBin function of Leaflet cannot incorporate the number of datapoints generated by methods I used. However, as addHexBin is developed and improved, it seems a promising way for managers to interact with their data directly. addHexBin allows GNOME output to be plotted in aggregate cells, similar to the figures presented here, on an html map, which users can zoom in and out of. The hexagonal cells update with the zoom level, allowing users to narrow in on specific problem areas. A Leaflet map that does not update with zoom level is achievable without addHexBin. addPolygons can be used to layer hexagons onto a map, showing the number of particles they contain when a cursor hovers over them.

Conclusion

While testing for FIB is a standard in determining water quality for shellfish growing areas, determining the source of FIB is a much more difficult task. I developed a method to (a) identify shoreline OSS at risk of leakage following inundation and (b) track the transport of FIB released from such OSS. This approach can help managers better understand sources and fates of FIB contamination as sea level rise increases the vulnerability of shoreline to storm surge and increases the threat of FIB contamination to shellfish growing areas. While the work presented here focused on Kitsap County, the methodology should be replicable throughout Puget Sound to safeguard the culturally and economically important resource of shellfish in the region.

Acknowledgements

This thesis would not have been possible without the help and kindness of many people. First, I would like to thank my committee. Dr. Terrie Klinger, my chair and advisor throughout my time at SMEA, provided the best and most thorough editing I have had in my academic career, as well as a wealth of expertise in the marine ecology of the region. She remained kind and steadfast throughout the ups and downs of my time at SMEA. Dr. Sunny Jardine, particularly through her spatial analysis class, was critical to the improvement of my skills in R; she also provided key feedback on this thesis.

Members of the Washington Department of Health have been so supportive throughout this process, from the early days of deciding what this project would look like, to teaching me key septic system and shellfish harvest information for the region, to giving me the opportunity to present my work to Washington Pollution Identification and Correction (PIC) managers. A specific thank you to Laura Johnson, Jeremy Simmons, Scott Berbells, Marnie Boardman, and Paula Reeves for being my main points of contact; Lea Shields for organizing the PIC meeting; and Roger Parker for providing important feedback on the relative risk levels of different OSS.

Two current and past members of the Kitsap Public Health District were also instrumental to this work. Grant Holdcroft took the time to have a long Zoom chat with me, sharing his expertise about OSS in Kitsap County and giving feedback on my overall methods. Anish Adhikari took the time to compile OSS data for me from the Kitsap County database.

Thank you to Kirsten Feifel of Puget Sound Partnership, who talked with me the summer after my second year and was willing to partner with me on this project to make me eligible for a grant opportunity. Her kindness and advice during that summer are much appreciated.

Dr. Ian Miller of Washington Sea Grant and Dr. Tarang Khangaonkar of Pacific Northwest National Laboratory provided sea level rise and Puget Sound oceanographic modeling data that were central to this thesis. They also took time to chat with me over Zoom and answer questions over email as I learned what this model data signified.

Thank you to SMEA and the Cooperative Institute for Climate, Ocean, & Ecosystem Studies (CICOES) for providing funding for my thesis. I am deeply grateful for receiving the following grants from the two: the SMEA Top Scholar Award (S. D. and B. F. Campbell Maritime Studies Endowed Fund; Hewlett Endowed Fund for Environmental Studies and Marine Affairs); the T. M. Leschine and K. O'Neill Endowment in Marine and Environmental Affairs; and the Cooperative Institute for Climate, Ocean, and Ecosystem Studies (CICOES) Graduate Student Fellowship.

Finally, a deep thank you to friends, both at SMEA and beyond, and family for uplifting me throughout my masters. This one is for you!

References

Allen, T. R., Crawford, T., Montz, B., Whitehead, J., Lovelace, S., Hanks, A. D., Christensen, A. R., & Kearney, G. D. (2019). Linking Water Infrastructure, Public Health, and Sea Level Rise: Integrated Assessment of Flood Resilience in Coastal Cities. *Public Works Management & Policy*, *24*(1), 110–139. https://doi.org/10.1177/1087724X18798380

Anderson, K. L., Whitlock, J. E., & Harwood, V. J. (2005). Persistence and Differential Survival of Fecal Indicator Bacteria in Subtropical Waters and Sediments. *Applied and Environmental Microbiology*, *71*(6), 3041–3048. https://doi.org/10.1128/AEM.71.6.3041-3048.2005

Bolster, C. H., Bromley, J. M., & Jones, S. H. (2005). Recovery of Chlorine-Exposed *Escherichia coli* in Estuarine Microcosms. *Environmental Science & Technology*, *39*(9), 3083–3089. https://doi.org/10.1021/es048643s

Cahoon, L. B., Hales, J. C., Carey, E. S., Loucaides, S., Rowland, K. R., & Nearhoof, J. E. (2006). Shellfishing Closures in Southwest Brunswick County, North Carolina: Septic Tanks vs. Storm-Water Runoff as Fecal Coliform Sources. *Journal of Coastal Research*, *22*(2), 319–327.

Campos, C. J. A., & Lees, D. N. (2014). Environmental Transmission of Human Noroviruses in Shellfish Waters. *Applied and Environmental Microbiology*, *80*(12), 3552–3561. https://doi.org/10.1128/AEM.04188-13

Chinnadurai, S., Campos, C. J. A., Geethalakshmi, V., Sharma, J., Kripa, V., & Mohamed, K. S. (2020). Microbiological quality of shellfish harvesting areas in the Ashtamudi and Vembanad estuaries (India): Environmental influences and compliance with international standards. *Marine Pollution Bulletin*, *156*, 111255. https://doi.org/10.1016/j.marpolbul.2020.111255

Cooper, J. A., Loomis, G. W., & Amador, J. A. (2016). Hell and High Water: Diminished Septic System Performance in Coastal Regions Due to Climate Change. *PLOS ONE*, *11*(9), e0162104. https://doi.org/10.1371/journal.pone.0162104

Coulliette, A. D., Money, E. S., Serre, M. L., & Noble, R. T. (2009). Space/Time Analysis of Fecal Pollution and Rainfall in an Eastern North Carolina Estuary. *Environmental Science & Technology*, 43(10), 3728–3735. https://doi.org/10.1021/es803183f

Cox, A. H., Dowling, M. J., Loomis, G. W., Engelhart, S. E., & Amador, J. A. (2020). Geospatial Modeling Suggests Threats from Stormy Seas to Rhode Island's Coastal Septic Systems. *Journal of Sustainable Water in the Built Environment*, *6*(3), 04020012. https://doi.org/10.1061/JSWBAY.0000917

Craft3. (n.d.). "Clean Water Loans." Accessed March 27, 2022. https://www.craft3.org/Borrow/clean-water-loans

Engie, K., & Klinger, T. (2007). Modeling passive dispersal through a large estuarine system to evaluate marine reserve network connections. Estuaries and Coasts, 30(2), 201–213. https://doi.org/10.1007/BF02700164

Graul, C. (2016). leafletR: Interactive Web-Maps Based on the Leaflet JavaScript Library. R package version 0.4-0, http://cran.r-project.org/package=leafletR

Hoghooghi, N., Pippin, J. S., Meyer, B. K., Hodges, J. B., & Bledsoe, B. P. (2021). Frontiers in assessing septic systems vulnerability in coastal Georgia, USA: Modeling approach and management implications. *PLOS ONE*, *16*(8), e0256606. https://doi.org/10.1371/journal.pone.0256606

Hummel, M. A., Berry, M. S., & Stacey, M. T. (2018). Sea Level Rise Impacts on Wastewater Treatment Systems Along the U.S. Coasts. *Earth's Future*, *6*(4), 622–633. https://doi.org/10.1002/2017EF000805

King County Department of Natural Resources and Parks, Wastewater Treatment Division. (2020). West Point Emergency Bypass Beach Closure Analysis and Simulation Report. Draft.

Kitsap County. (2020). Climate Change Resiliency Assessment. https://www.kitsapgov.com/dcd/Kitsap_climate_assessment/KitsapCountyClimateAssessment_June2020%20-%202%20Full%20Assessment%20LowRes.pdf#page=78&zoom=100,92,96

Kitsap Public Health District. (n.d.1). "Septic Systems." Accessed March 27, 2022. https://kitsappublichealth.org/environment/septic_systems.php

Kitsap Public Health District. (n.d.2). Homeowners Guide to Onsite Sewage Systems. Accessed June 3, 2022. https://kitsappublichealth.org/information/files/resources/EH-10.pdf

Lipp, E. K., Kurz, R., Vincent, R., Rodriguez-Palacios, C., Farrah, S. R., & Rose, J. B. (2001). The Effects of Seasonal Variability and Weather on Microbial Fecal Pollution and Enteric Pathogens in a Subtropical Estuary. *Estuaries*, *24*(2), 266. https://doi.org/10.2307/1352950

Lizárraga-Partida, M. L., & Cárdenas, G. V. (1996). Influence of water circulation on marine and faecal bacteria in a mussel-growing area. *Marine Pollution Bulletin*, *32*(2), 196–201. https://doi.org/10.1016/0025-326X(95)00119-8

Martínez, O., Rodríguez-Calleja, J. M., Santos, J. A., Otero, A., & García-López, M. L. (2009). Foodborne and Indicator Bacteria in Farmed Molluscan Shellfish before and after Depuration. *Journal of Food Protection*, *72*(7), 1443–1449. https://doi.org/10.4315/0362-028X-72.7.1443

Miller, I.M., Mastriani, E. (2017). Prioritizing Flood Risk Reduction and Ecosystem Services on the Dungeness River Delta: A Parcel Scale Analysis. A collaboration with the Jamestown S'Klallam Tribe. Released 11/2017.

Miller, I.M., Morgan, H., Mauger, G., Newton, T., Weldon, R., Schmidt, D., Welch, M., Grossman, E. (2018). Projected Sea Level Rise for Washington State – A 2018 Assessment. A collaboration of Washington Sea Grant, University of Washington Climate Impacts Group, University of Oregon, University of Washington, and US Geological Survey. Prepared for the Washington Coastal Resilience Project. Updated 07/2019.

Miller, I.M., Yang, Z., VanArendonk, N., Grossman, E., Mauger, G. S., Morgan, H. (2019). Extreme Coastal Water Level in Washington State: Guidelines to Support Sea Level Rise Planning. A collaboration of Washington Sea Grant, University of Washington Climate Impacts Group, Oregon State University, University of Washington, Pacific Northwest National Laboratory and U.S. Geological Survey. Prepared for the Washington Coastal Resilience Project.

Moore, S. K., Mantua, N. J., Newton, J. A., Kawase, M., Warner, M. J., & Kellogg, J. P. (2008). A descriptive analysis of temporal and spatial patterns of variability in Puget Sound oceanographic properties. *Estuarine, Coastal and Shelf Science*, *80*(4), 545–554. https://doi.org/10.1016/j.ecss.2008.09.016

Perri, K. A., Sullivan, J. M., & Boyer, G. L. (2015). Harmful algal blooms in Sodus Bay, Lake Ontario: A comparison of nutrients, marina presence, and cyanobacterial toxins. *Journal of Great Lakes Research*, *41*(2), 326–337. https://doi.org/10.1016/j.jglr.2015.03.022

Puget Sound Partnership (PSP). (2021). "Shoreline Armoring." https://vitalsigns.pugetsoundinfo.wa.gov/VitalSign/Detail/16

R Core Team. (2022). R: A language and environment for statistical computing. R Foundation for Statistical Computing, Vienna, Austria. URL http://www.R-project.org/.

Raymond, C.L, Faghin, N., Morgan, H., and Roop, H. (2020). How to Choose: A Primer for Selecting Sea Level Rise Projections for Washington State. A collaboration of Washington Sea Grant and University of Washington Climate Impacts Group. Prepared for the Washington Coastal Resilience Project.

Schulz, C. J., & Childers, G. W. (2011). Fecal Bacteroidales Diversity and Decay in Response to Variations in Temperature and Salinity. *Applied and Environmental Microbiology*, *77*(8), 2563–2572. https://doi.org/10.1128/AEM.01473-10

Seattle and King County Public Health (n.d.). "Homeowner's Septic System Manual." https://kingcounty.gov/depts/health/environmental-health/piping/onsite-sewage-systems/brochures.aspx

Shehane, S. D., Harwood, V. J., Whitlock, J. E., & Rose, J. B. (2005). The influence of rainfall on the incidence of microbial faecal indicators and the dominant sources of faecal pollution in a Florida river. *Journal of Applied Microbiology*, *98*(5), 1127–1136. https://doi.org/10.1111/j.1365-2672.2005.02554.x

Simmons, R. C., McNamara, D., & Keller, H. (2018). "Understanding shoreline landowner views on water quality best management practices and outreach." 2018 Salish Sea Ecosystem Conference presentation.

Sinton, L., Hall, C., & Braithwaite, R. (2007). Sunlight inactivation of Campylobacter jejuni and Salmonella enterica, compared with Escherichia coli, in seawater and river water. *Journal of Water and Health*, *5*(3), 357–365. https://doi.org/10.2166/wh.2007.031

TCW Economics. (2008). "Economic analysis of the non-treaty commercial and recreational fisheries in Washington State." Sacramento, CA. With technical assistance from The Research Group, Corvallis, OR.

U.S. Census Bureau (2019). Annual Estimates of the Resident Population for Counties in Washington: April 1, 2010 to July 1, 2019 (CO-EST2019-ANNRES-53). https://www.census.gov/data/datasets/time-series/demo/popest/2010s-counties-total.html#par_textimage_739801612

U.S. Environmental Protection Agency (EPA). (n.d.). "Septic Systems Overview." https://www.epa.gov/septic/septic-systems-overview

U.S. v. Washington, 384 F. Supp. 312 (U.S. District Court for the Western District of Washington 1974). https://cite.case.law/f-supp/384/312/

U.S. v. Washington, 873 Supp. 1422 (U.S. District Court for the Western District of Washington 1994). https://law.justia.com/cases/federal/district-courts/FSupp/873/1422/1466184/

U.S. v. Washington, No. 13-35474 (U.S. Court of Appeals for the Ninth Circuit 2017). https://law.justia.com/cases/federal/appellate-courts/ca9/13-35474/13-35474-2017-05-19.html

Van Vuuren, D. P., Edmonds, J., Kainuma, M., Riahi, K., Thomson, A., Hibbard, K., Hurtt, G. C., Kram, T., Krey, V., Lamarque, J.-F., Masui, T., Meinshausen, M., Nakicenovic, N., Smith, S. J., & Rose, S. K. (2011). The representative concentration pathways: An overview. *Climatic Change*, *109*(1), 5. https://doi.org/10.1007/s10584-011-0148-z

Washington Department of Health (WA DOH). (n.d.1). "About the Shellfish Growing Areas Program". Accessed March 26, 2022. https://doh.wa.gov/about-us/programs-and-

services/environmental-public-health/environmental-health-and-safety/about-shellfish-program/about-shellfish-growing-areas-program

Washington Department of Health (WA DOH). (n.d.2). "Large On-Site Sewage Systems (LOSS)." Accessed March 17, 2022. https://doh.wa.gov/community-and-environment/wastewater-management/loss-program

Yang, Z., & Khangaonkar, T. (2010). Multi-scale modeling of Puget Sound using an unstructured-grid coastal ocean model: From tide flats to estuaries and coastal waters. *Ocean Dynamics*, *60*(6), 1621–1637. https://doi.org/10.1007/s10236-010-0348-5

Yang, Z., Wang, T., Castrucci, L. (2019). Storm Surge Modeling in Puget Sound. Pacific Northwest National Laboratory. Prepared for the US Department of Energy.

Zelenke, B., C. O'Connor, C. Barker, C.J. Beegle-Krause, and L. Eclipse (Eds.). (2012). General NOAA Operational Modeling Environment (GNOME) Technical Documentation. *U.S. Dept. of Commerce, NOAA Technical Memorandum NOS OR&R 40*. Seattle, WA: Emergency Response Division, NOAA. 105 pp. http://response.restoration.noaa.gov/gnome_manual

Tables

Septic Type	WA DOH Pre-Treatment Level	Risk Level	Number on Kitsap County Shoreline
Large Onsite Sewage System (LOSS)	N/A	1	3
Glendon	A	2	270
Aerobic	A with UV treatment, B without UV treatment	2	397
Sand Filter	B	2	157
Bottomless Sand Filter	B	2	60
Oscar Low eFlow	B	2	7
Packed Bed Filter	B	2	6
Mound	B with 2 feet of sand/ C with 1 foot of sand	3	29
Pressure System	C	3	278
Standard Gravity	E	5	1512
Pump-To-Gravity	E	5	559
Gravity With Reduction	E	5	1
Holding Tank	E	5	7
Septic – No Permit	N/A	6	406
Septic – No Records	N/A	6	135
Other	N/A	6	8
Undetermined	N/A	6	1105

Table 1. Shoreline OSS of Kitsap County on parcels projected to be inundated with three feet of sea level rise. Vulnerability was assessed originally through the work of Miller et al. (2017), who collaborated with Clallam County staff. Vulnerability rankings were refined through conversations with the Washington Department of Health and Kitsap Public Health District. There were no OSS in this dataset of a type that Washington Department of Health classifies "pre-treatment level D."

Figures

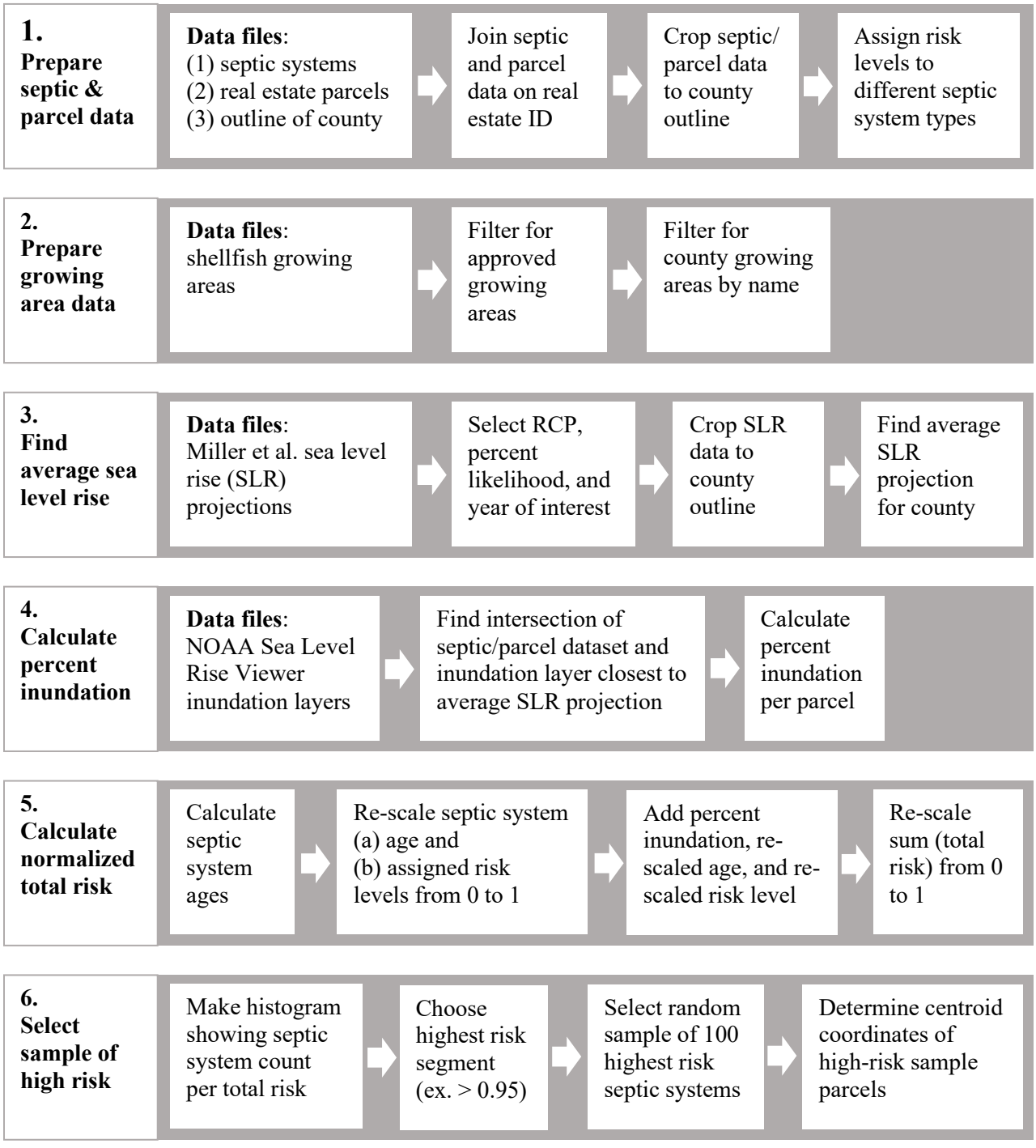
1. Prepare septic & parcel data
Data files: (1) septic systems (2) real estate parcels (3) outline of county
Join septic and parcel data on real estate ID
Crop septic/ parcel data to county outline
Assign risk levels to different septic system types
2. Prepare growing area data
Data files: shellfish growing areas
Filter for approved growing areas
Filter for county growing areas by name
3. Find average sea level rise
Data files: Miller et al. sea level rise (SLR) projections
Select RCP, percent likelihood, and year of interest
Crop SLR data to county outline
Find average SLR projection for county
4. Calculate percent inundation
Data files: NOAA Sea Level Rise Viewer inundation layers
Find intersection of septic/parcel dataset and inundation layer closest to average SLR projection
Calculate percent inundation per parcel
5. Calculate normalized total risk
Calculate septic system ages
Re-scale septic system (a) age and (b) assigned risk levels from 0 to 1
Add percent inundation, re-scaled age, and re-scaled risk level
Re-scale sum (total risk) from 0 to 1
6. Select sample of high risk
Make histogram showing septic system count per total risk
Choose highest risk segment (ex. > 0.95)
Select random sample of 100 highest risk septic systems
Determine centroid coordinates of high-risk sample parcels

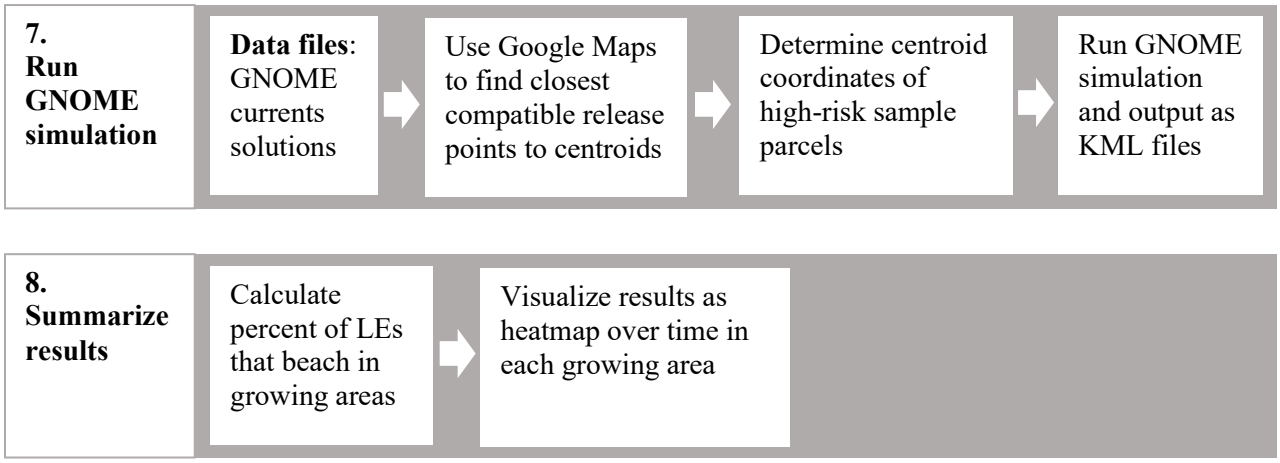

Figure 1. Overview of my methodology.

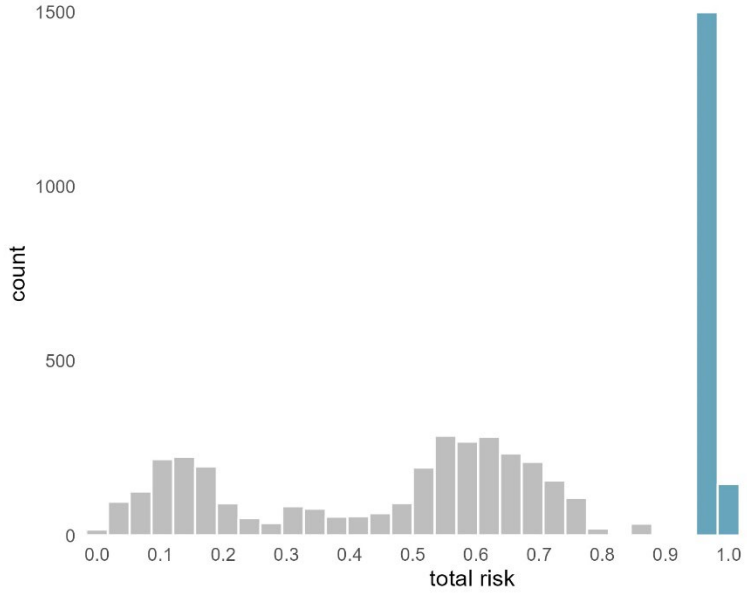

Figure 2. A histogram of total risk for each shoreline OSS in Kitsap County. OSS with a total risk higher than 0.95 are highlighted in blue.

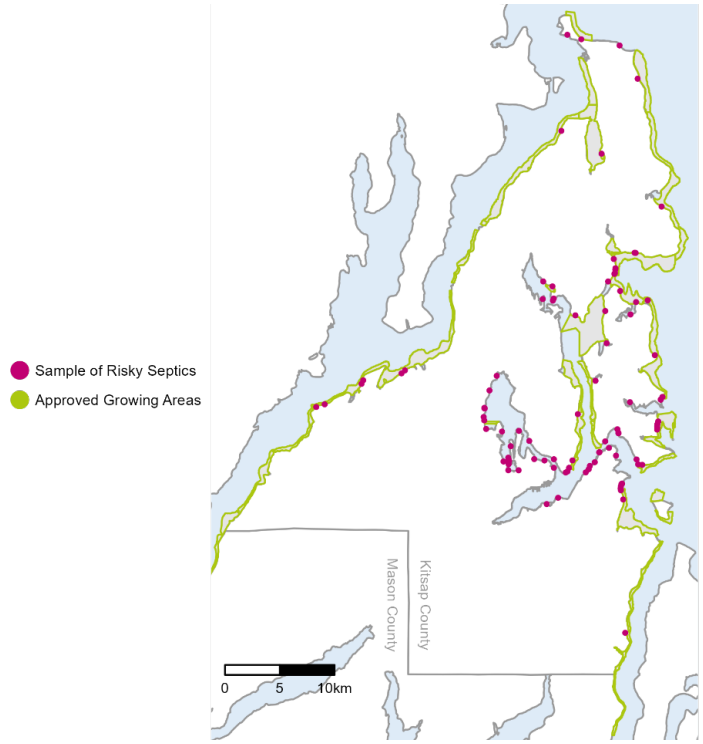

Figure 3. Spatial distribution of a sample of 100 OSS in Kitsap County, each with an individual total risk > 0.95, overlaid on shellfish growing areas currently approved by WA DOH. I determined total risk by adding three factors: (1) the percent area inundated of the real estate parcel on which the OSS is located under 4 feet of flooding, (2) the age of the OSS, and (3) the relative level of leakage that the type of OSS will produce during brief inundation of its drain field.

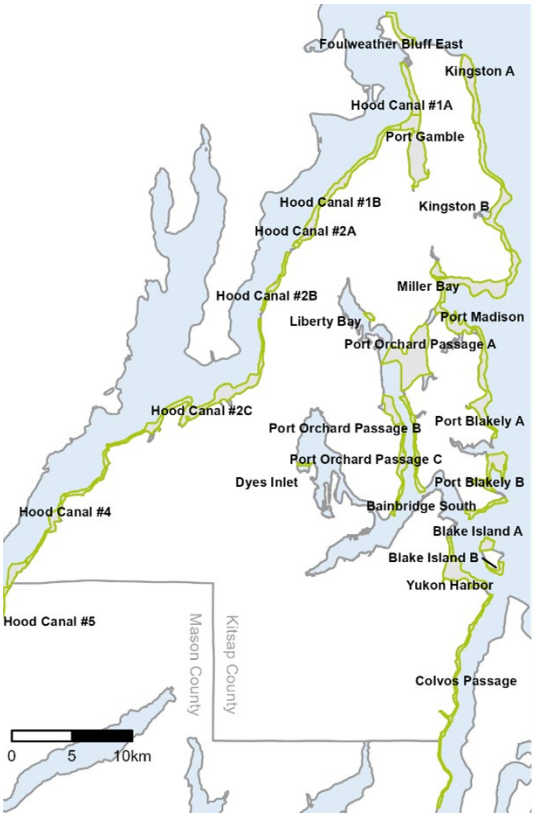

Figure 4. Locations of approved shellfish growing areas in Kitsap County. When multiple growing areas have the same name, I have assigned them a clarifying letter, which match their output in the following figures.

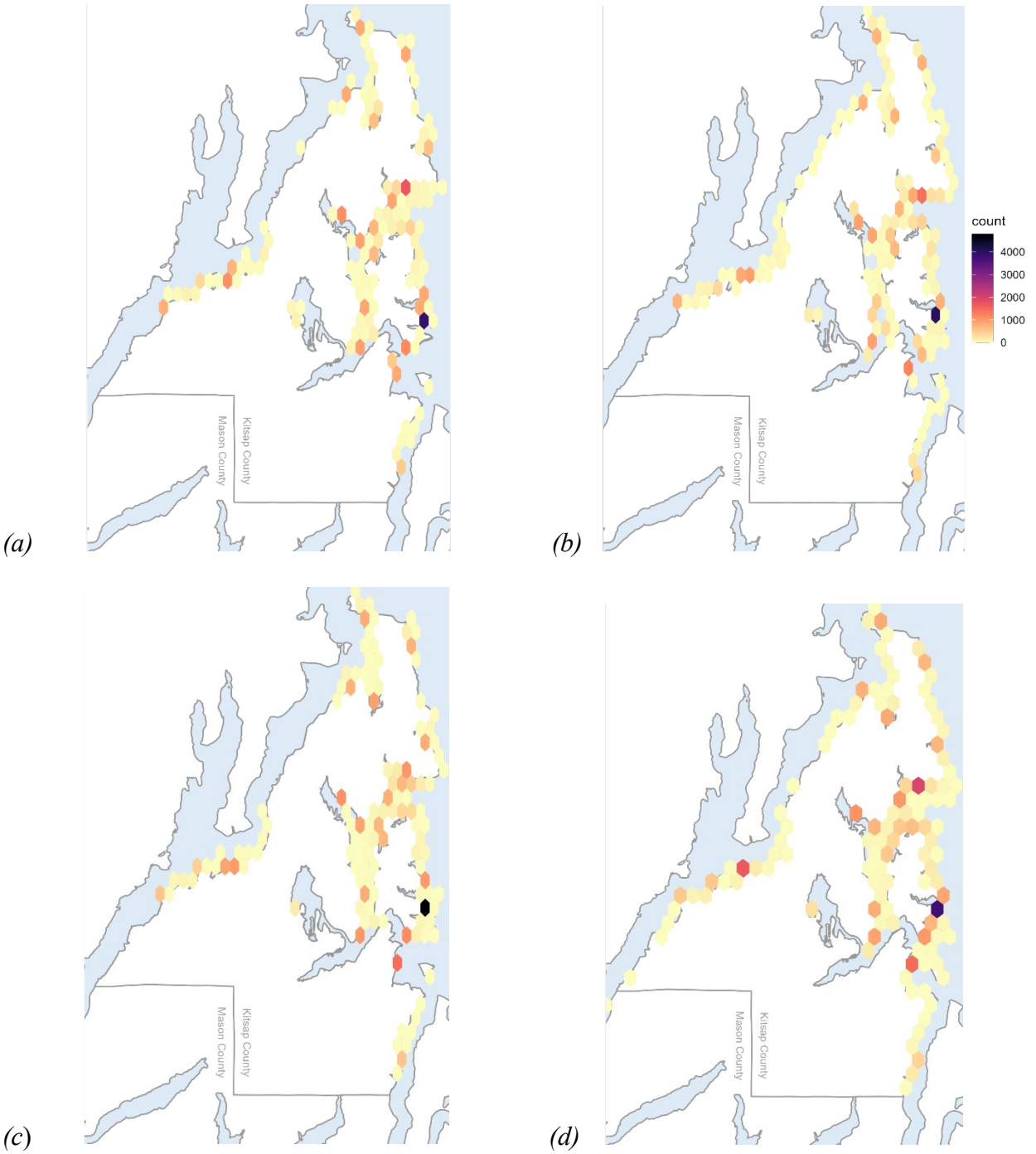

Figure 5. Simulated particle distributions across Kitsap County after 1 day (a) and 1 week (b) in the rainiest week of 2014, March 2-9, and after 1 day (c) and 1 week (d) in a driest week of 2014, September 3-10. Simulated spill lasted throughout the first 24 hours of spill. The legend in (b) applies to the coloring for all 4 scenarios.

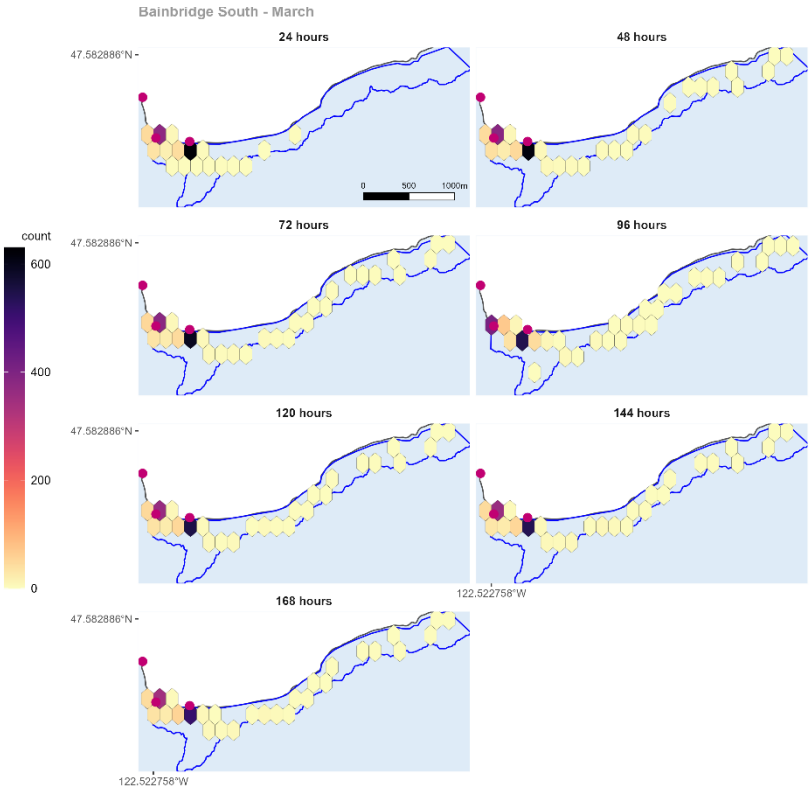

Figure 6. Simulated particle distributions in the Bainbridge South growing area for consecutive 24-hour time periods in March. The blue line shows the border of the approved growing area. Pink dots mark spill start points.

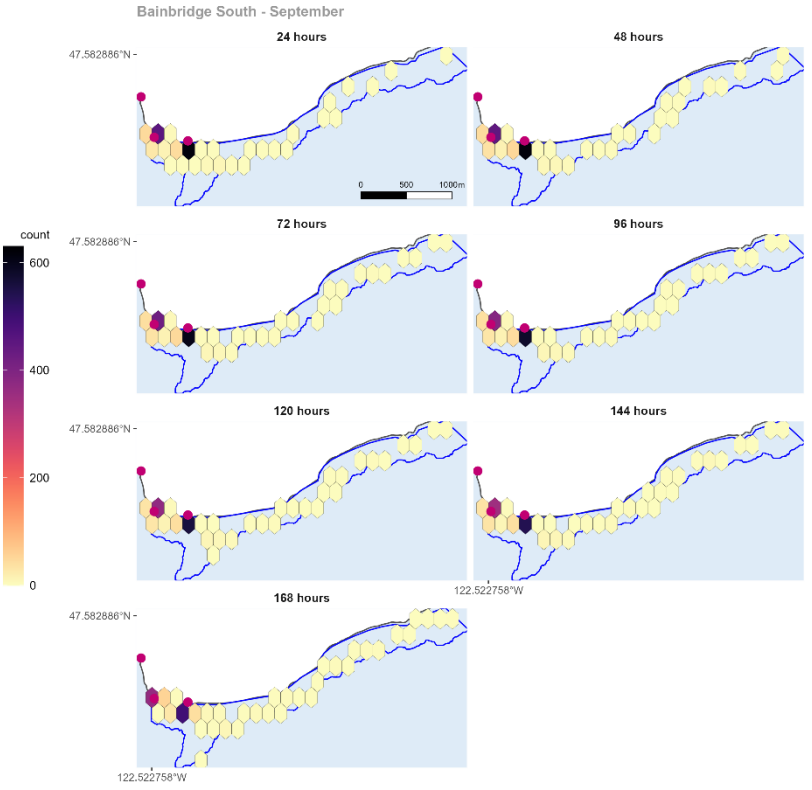

Figure 7. Simulated particle distributions in the Bainbridge South growing area for consecutive 24-hour time periods in September. The blue line shows the border of the approved growing area. Pink dots mark spill start points.

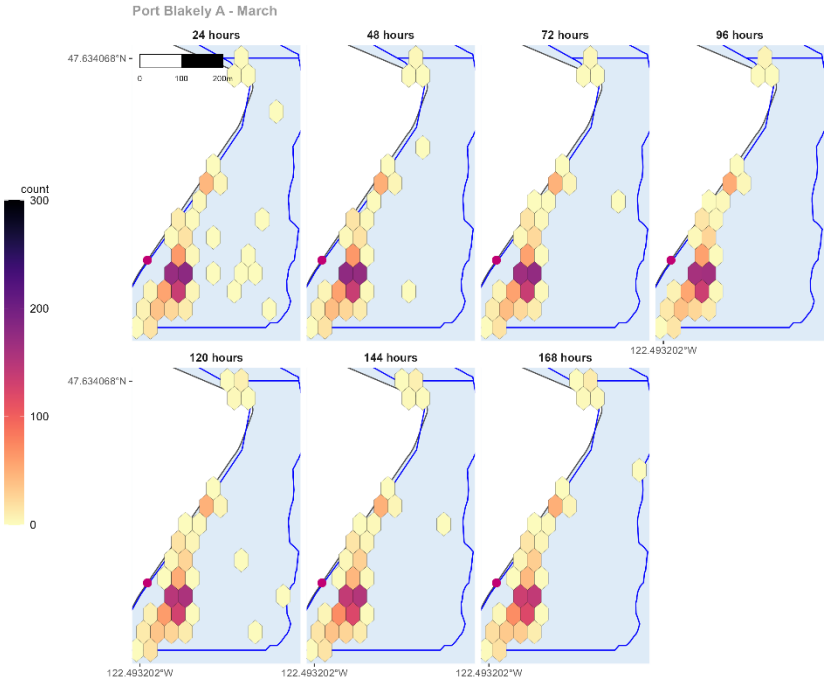

Figure 8. Simulated particle distributions in the Port Blakely A growing area for consecutive 24-hour time periods in March. The blue line shows the border of the approved growing area. Pink dots mark spill start points.

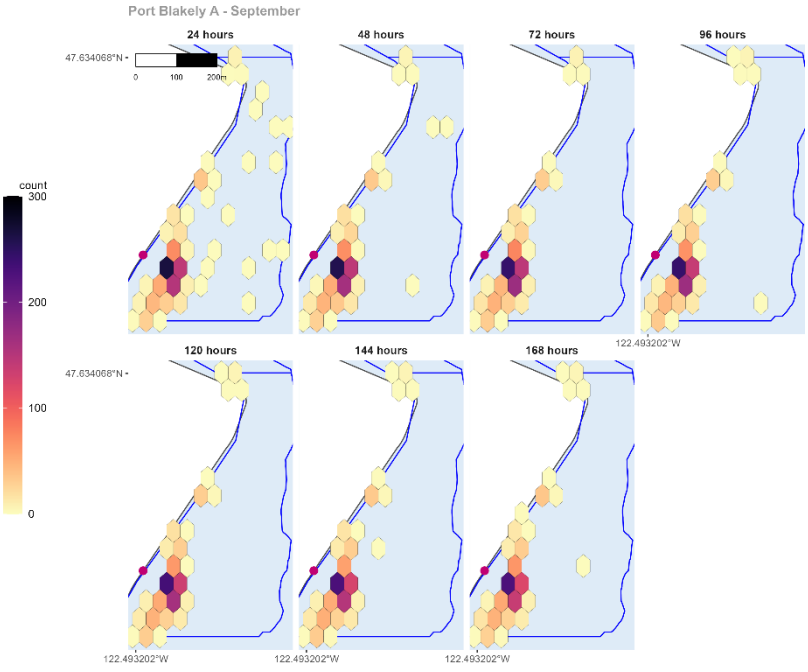

Figure 9. Simulated particle distributions in the Port Blakely A growing area for consecutive 24-hour time periods in September. The blue line shows the border of the approved growing area. Pink dots mark spill start points.

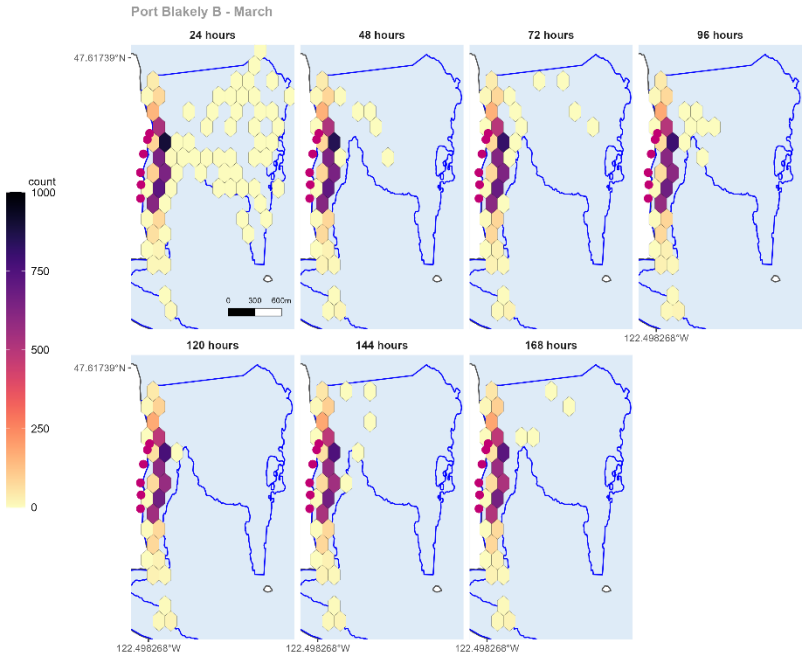

Figure 10. Simulated particle distributions in the Port Blakely B growing area for consecutive 24-hour time periods in March. The blue line shows the border of the approved growing area. Pink dots mark spill start points.

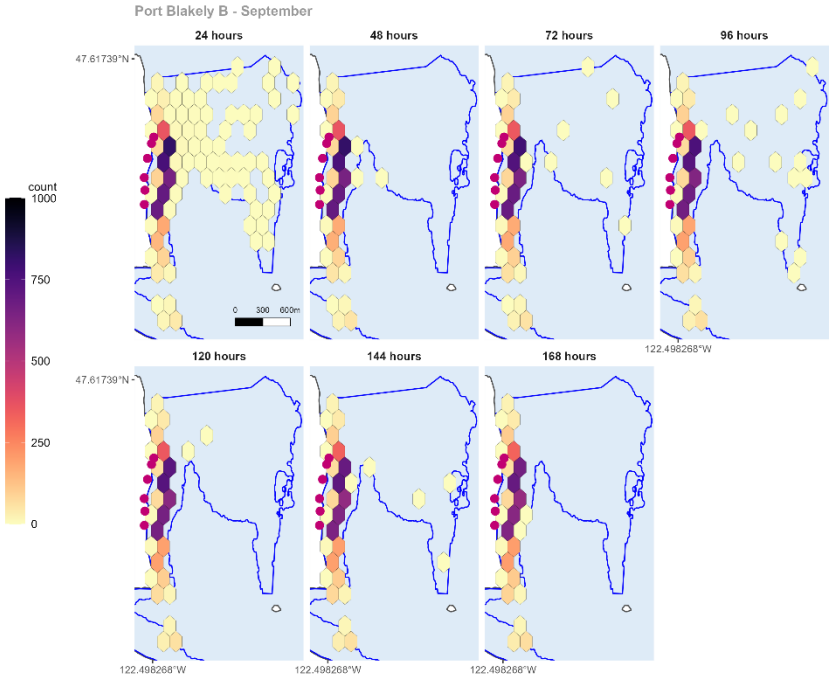

Figure 11. Simulated particle distributions in the Port Blakely B growing area for consecutive 24-hour time periods in September. The blue line shows the border of the approved growing area. Pink dots mark spill start points.

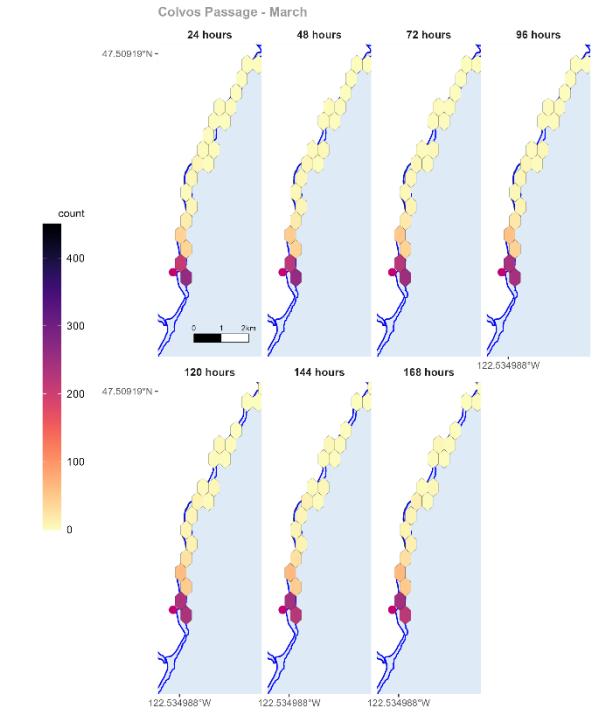

Figure 12. Simulated particle distributions in the Colvos Passage growing area for consecutive 24-hour time periods in March. The blue line shows the border of the approved growing area. Pink dots mark spill start points.

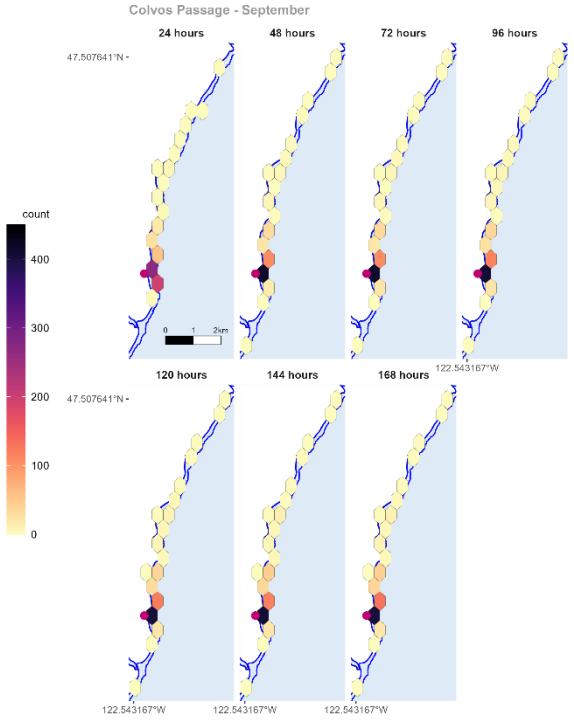

Figure 13. Simulated particle distributions in the Colvos Passage growing area for consecutive 24-hour time periods in September. The blue line shows the border of the approved growing area. Pink dots mark spill start points.

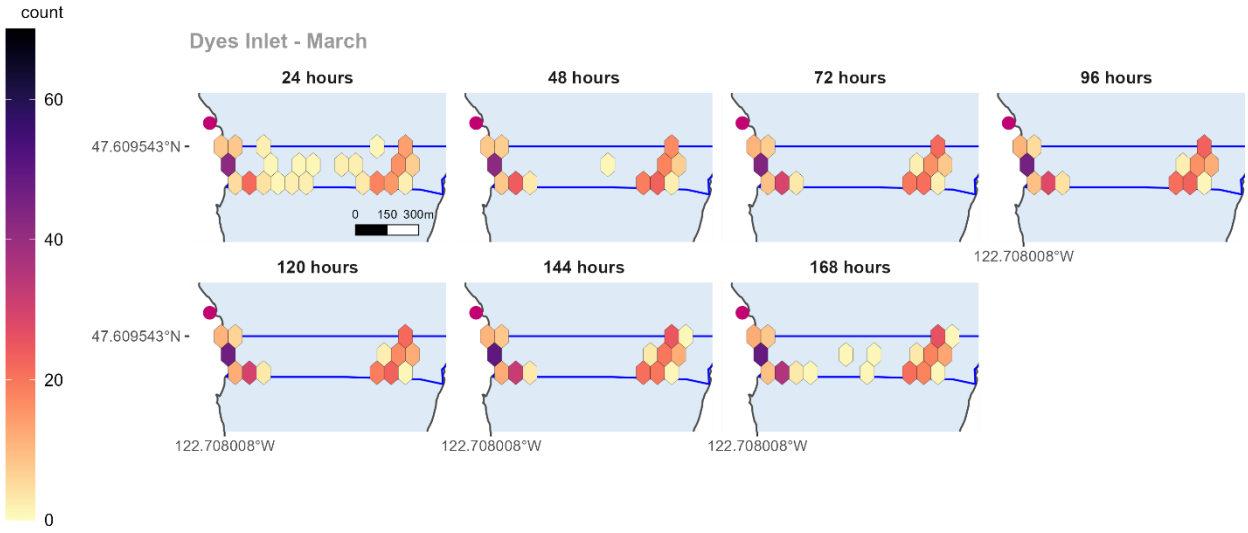

Figure 14. Simulated particle distributions in the Dyes Inlet growing area for consecutive 24-hour time periods in March. The blue line shows the border of the approved growing area. Pink dots mark spill start points.

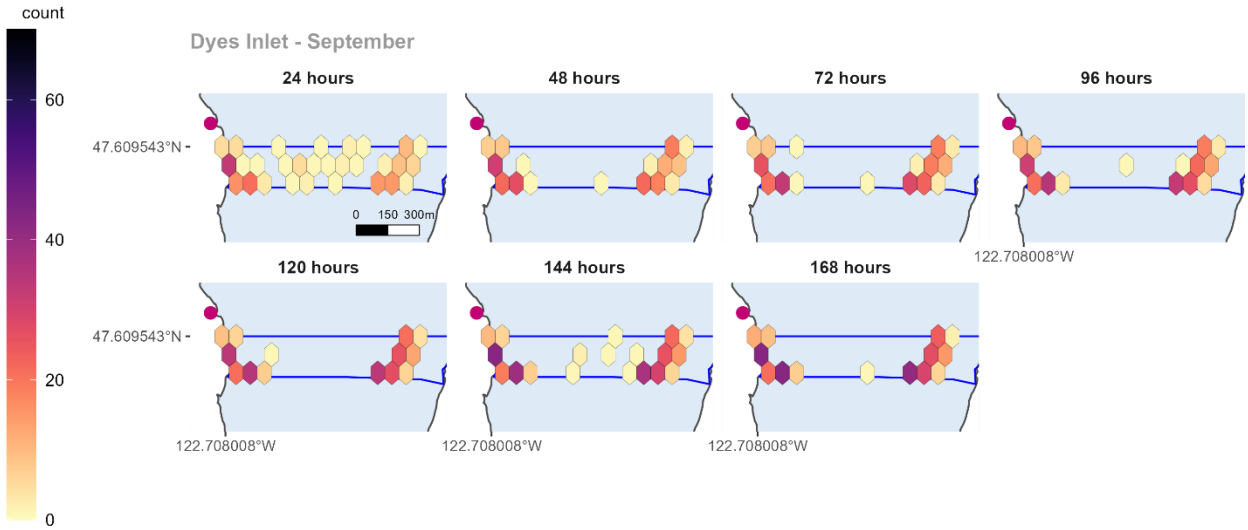

Figure 15. Simulated particle distributions in the Dyes Inlet growing area for consecutive 24-hour time periods in September. The blue line shows the border of the approved growing area. Pink dots mark spill start points.

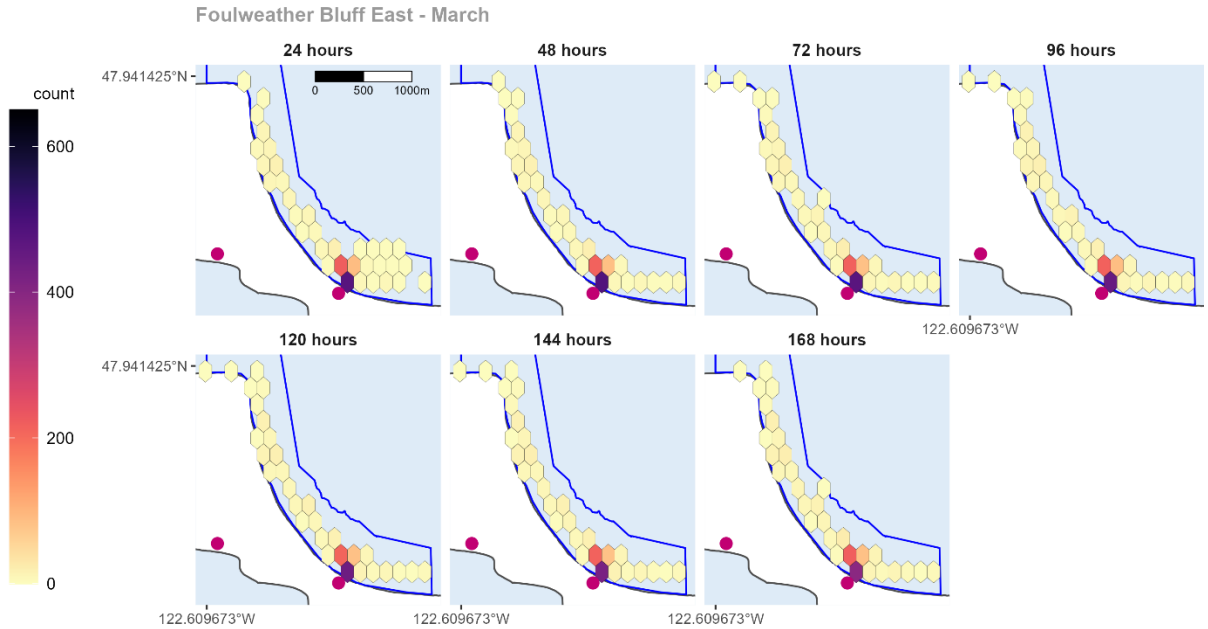

Figure 16. Simulated particle distributions in the Foulweather Bluff East growing area for consecutive 24-hour time periods in March. The blue line shows the border of the approved growing area. Pink dots mark spill start points. The lack of particles on the southwest corner of the figure exists only because the data is filtered to those within the Foulweather Bluff East growing area.

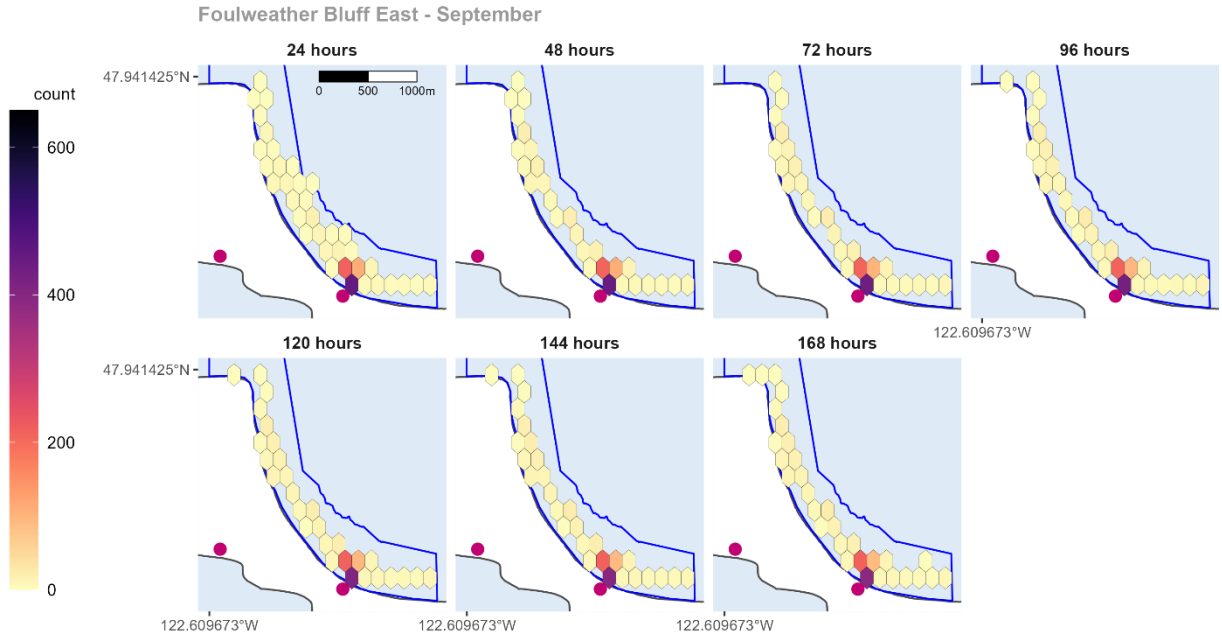

Figure 17. Simulated particle distributions in the Foulweather Bluff East growing area for consecutive 24-hour time periods in September. The blue line shows the border of the approved growing area. Pink dots mark spill start points. The lack of particles on the southwest corner of the figure exists only because the data is filtered to those within the Foulweather Bluff East growing area.

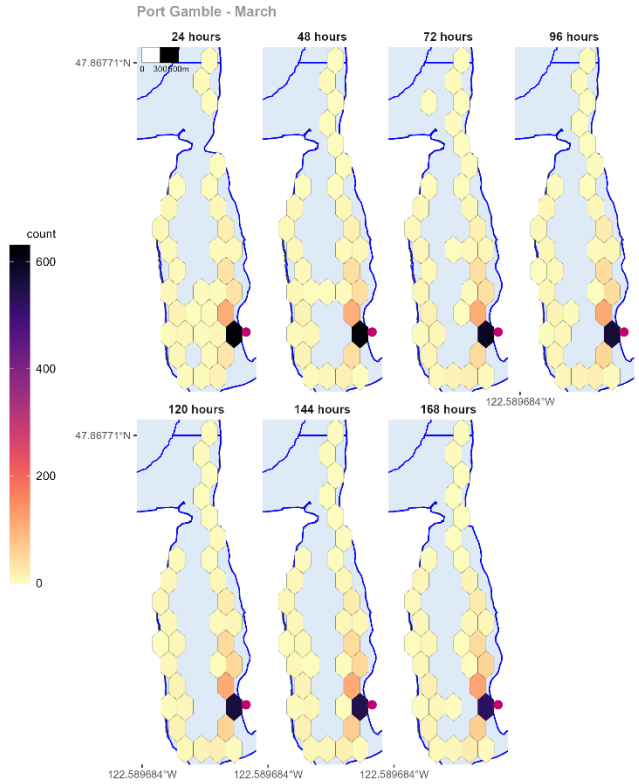

Figure 18. Simulated particle distributions in the Port Gamble growing area for consecutive 24-hour time periods in March. The blue line shows the border of the approved growing area. Pink dots mark spill start points.

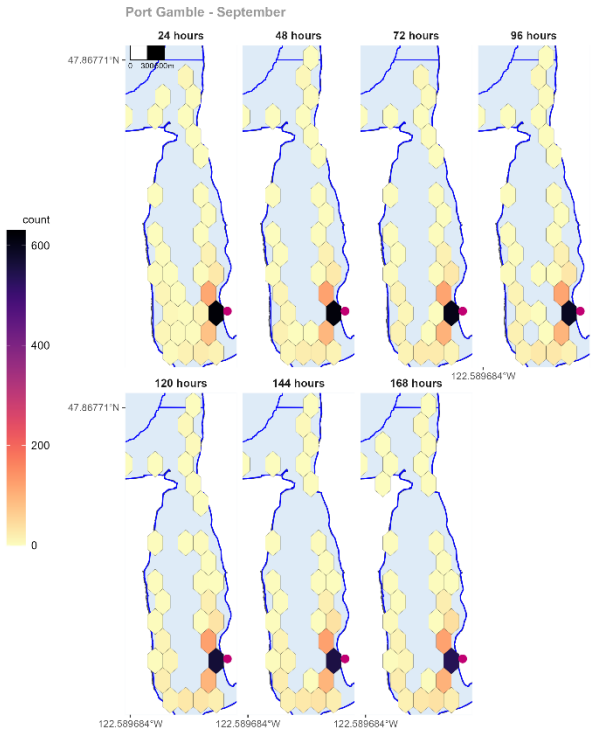

Figure 19. Simulated particle distributions in the Port Gamble growing area for consecutive 24-hour time periods in September. The blue line shows the border of the approved growing area. Pink dots mark spill start points.

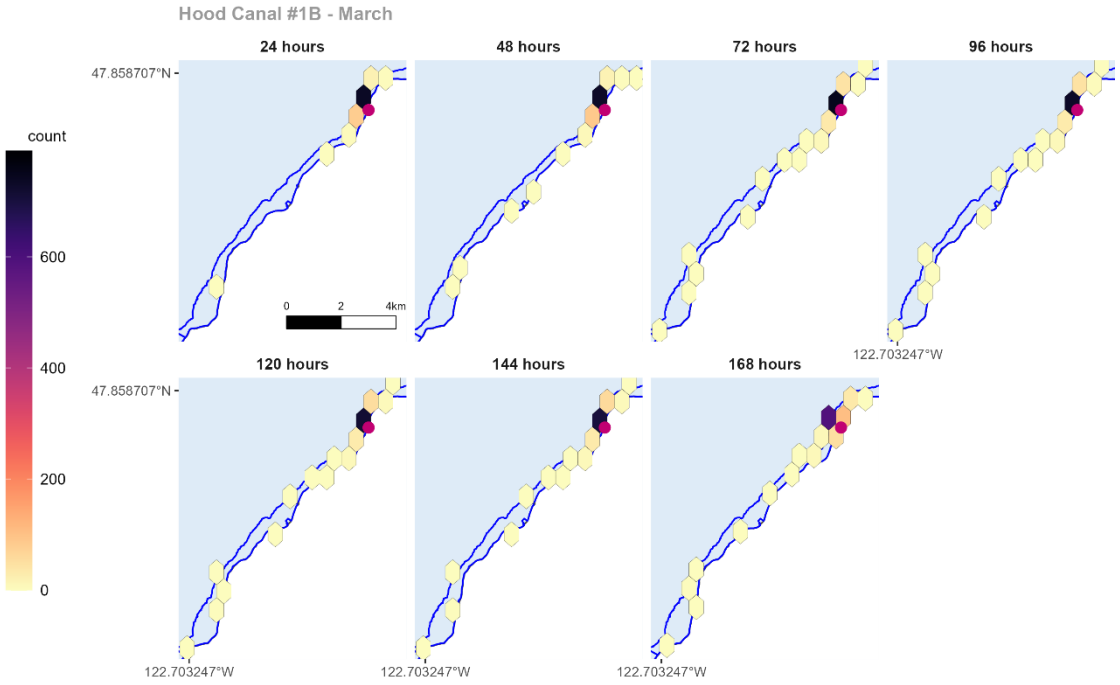

Figure 20. Simulated particle distributions in the Hood Canal #1B growing area for consecutive 24-hour time periods in March. The blue line shows the border of the approved growing area. Pink dots mark spill start points.

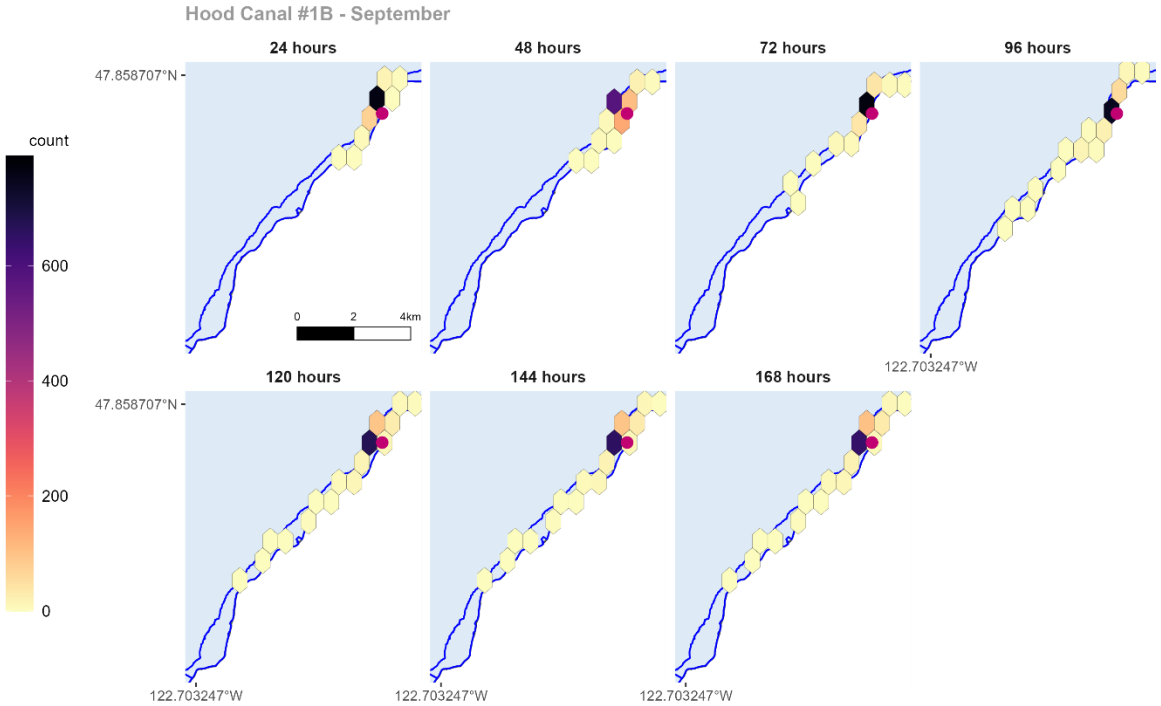

Figure 21. Simulated particle distributions in the Hood Canal #1B growing area for consecutive 24-hour time periods in September. The blue line shows the border of the approved growing area. Pink dots mark spill start points.

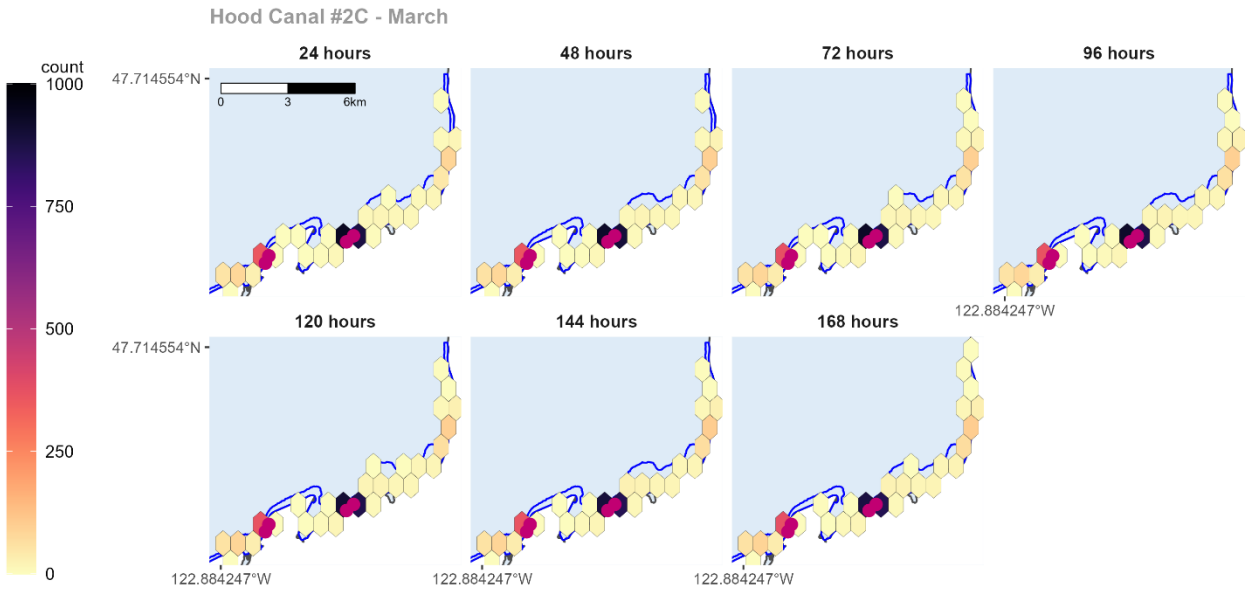

Figure 22. Simulated particle distributions in the Hood Canal #2C growing area for consecutive 24-hour time periods in March. The blue line shows the border of the approved growing area. Pink dots mark spill start points.

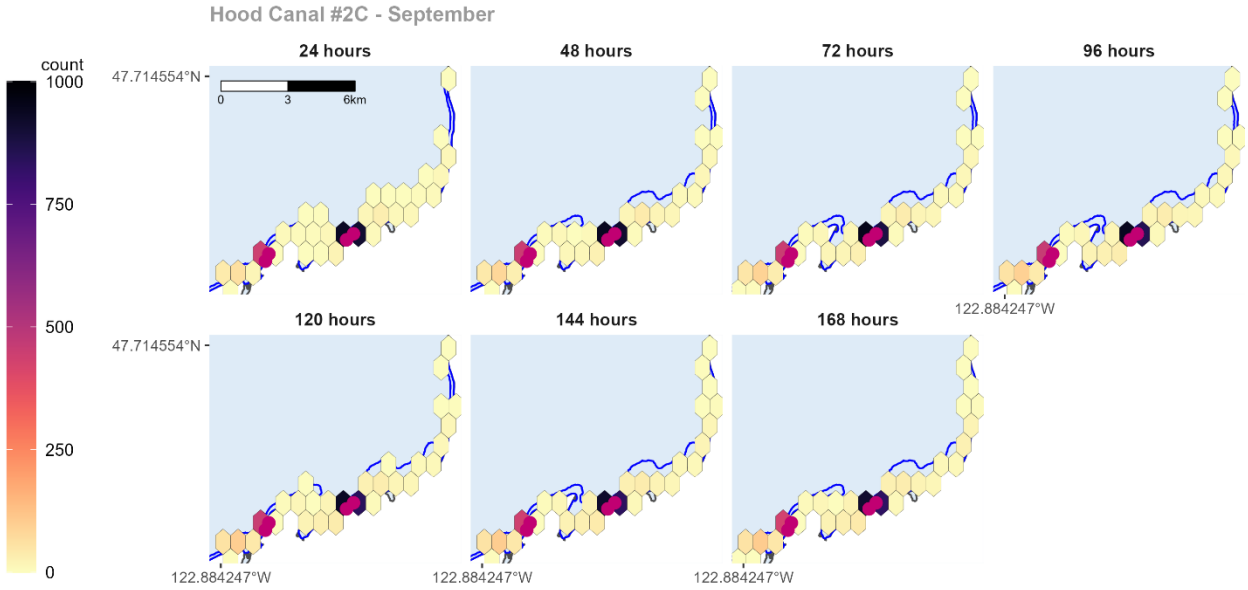

Figure 23. Simulated particle distributions in the Hood Canal #2C growing area for consecutive 24-hour time periods in September. The blue line shows the border of the approved growing area. Pink dots mark spill start points.

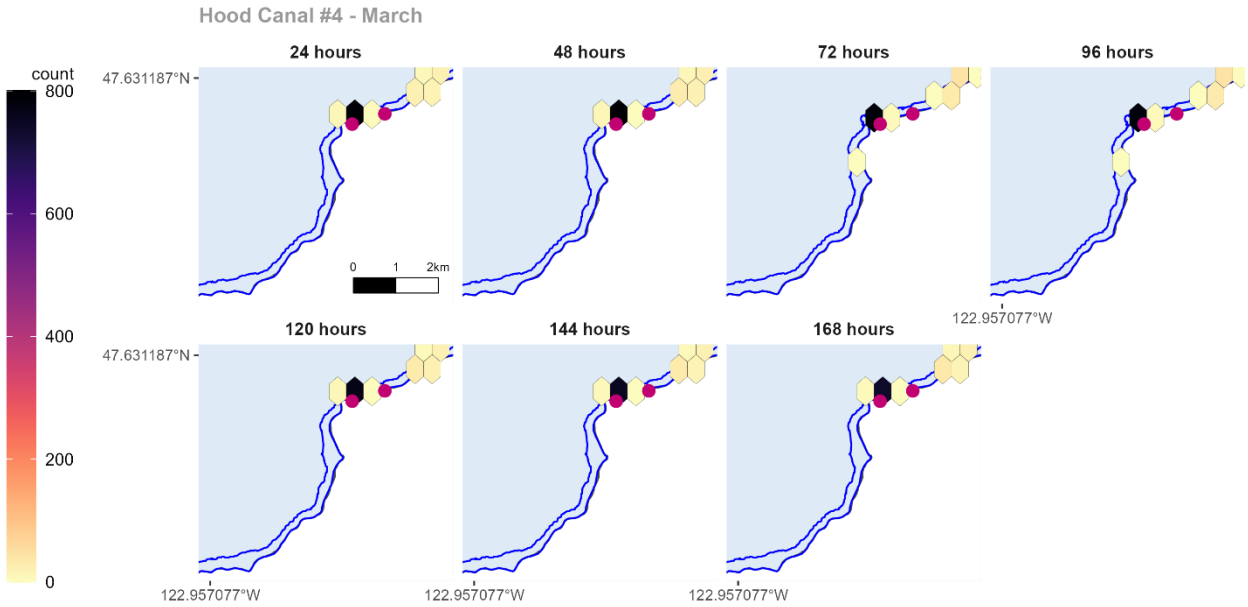

Figure 24. Simulated particle distributions in the Hood Canal #4 growing area for consecutive 24-hour time periods in March. The blue line shows the border of the approved growing area. Pink dots mark spill start points.

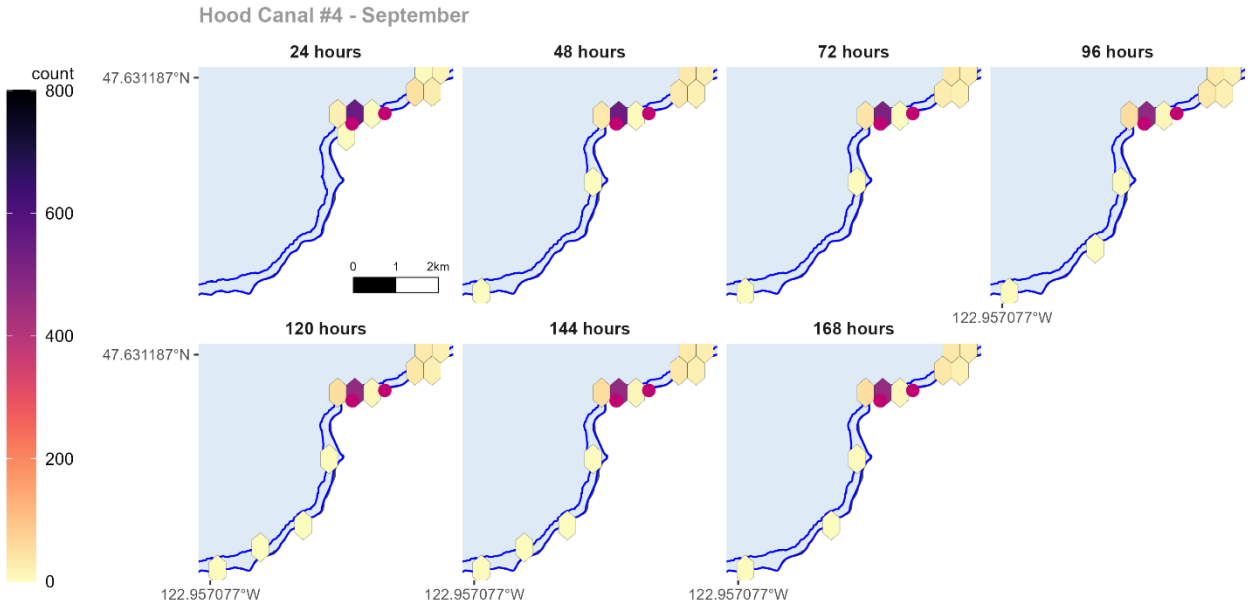

Figure 25. Simulated particle distributions in the Hood Canal #4 growing area for consecutive 24-hour time periods in September. The blue line shows the border of the approved growing area. Pink dots mark spill start points.

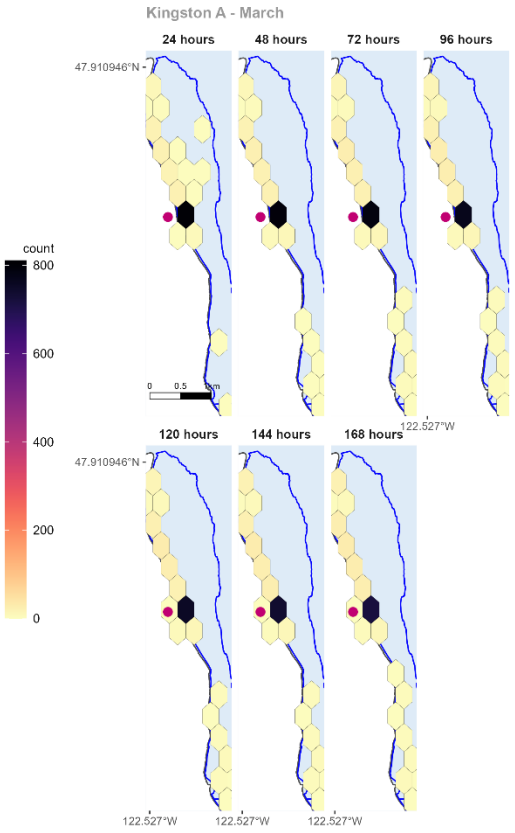

Figure 26. Simulated particle distributions in the Kingston A growing area for consecutive 24-hour time periods in March. The blue line shows the border of the approved growing area. Pink dots mark spill start points.

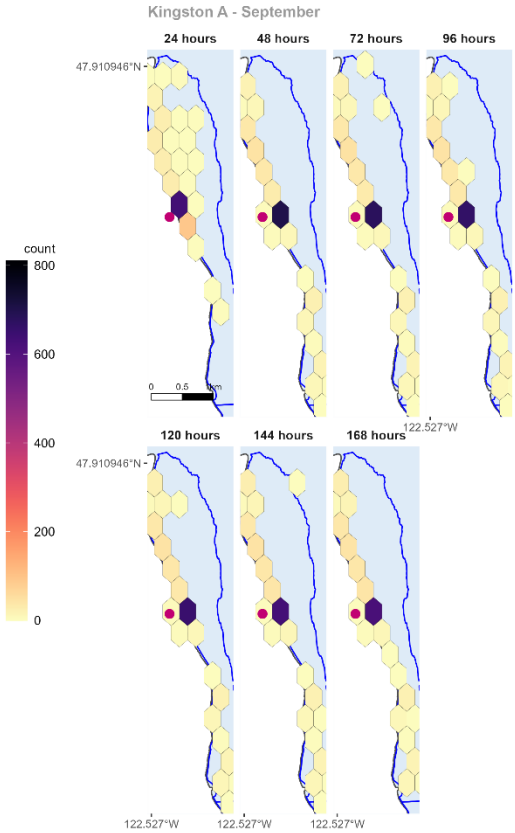

Figure 27. Simulated particle distributions in the Kingston A growing area for consecutive 24-hour time periods in September. The blue line shows the border of the approved growing area. Pink dots mark spill start points.

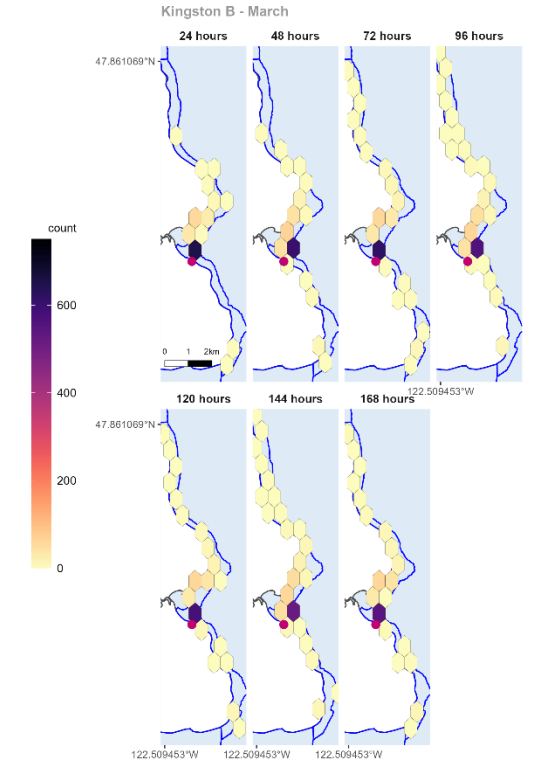

Figure 28. Simulated particle distributions in the Kingston B growing area for consecutive 24-hour time periods in March. The blue line shows the border of the approved growing area. Pink dots mark spill start points.

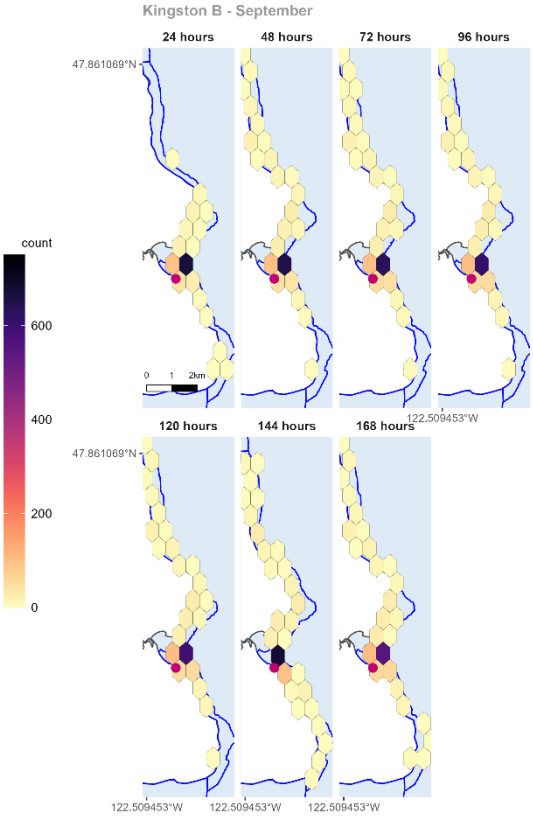

Figure 29. Simulated particle distributions in the Kingston B growing area for consecutive 24-hour time periods in September. The blue line shows the border of the approved growing area. Pink dots mark spill start points.

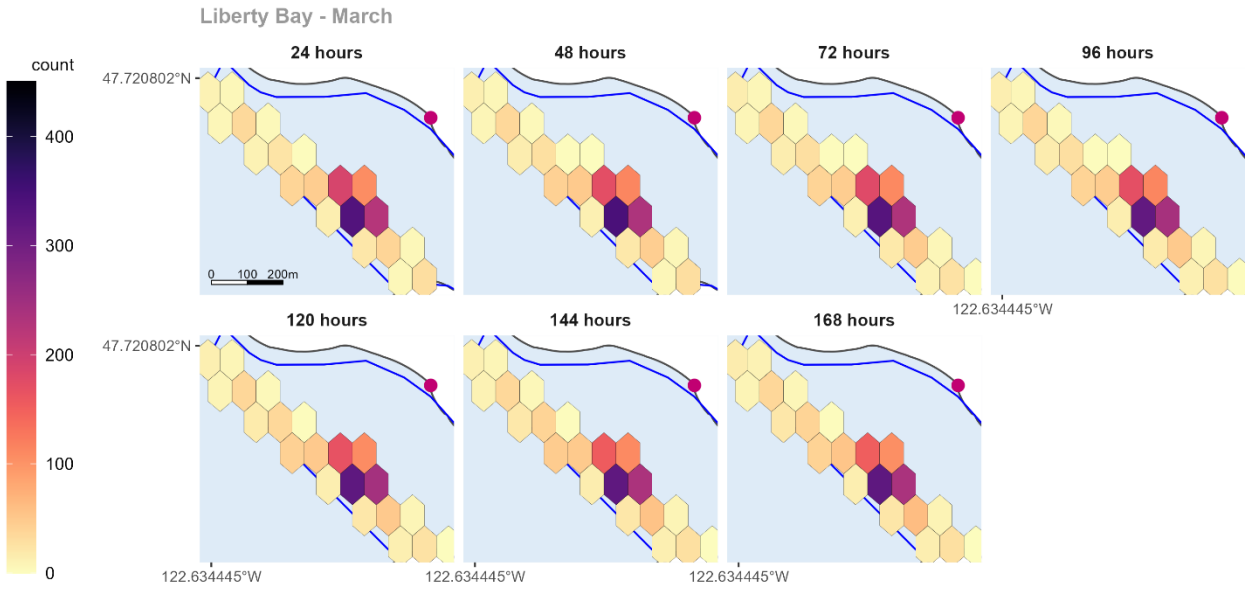

Figure 30. Simulated particle distributions in the Liberty Bay growing area for consecutive 24-hour time periods in March. The blue line shows the border of the approved growing area. Pink dots mark spill start points.

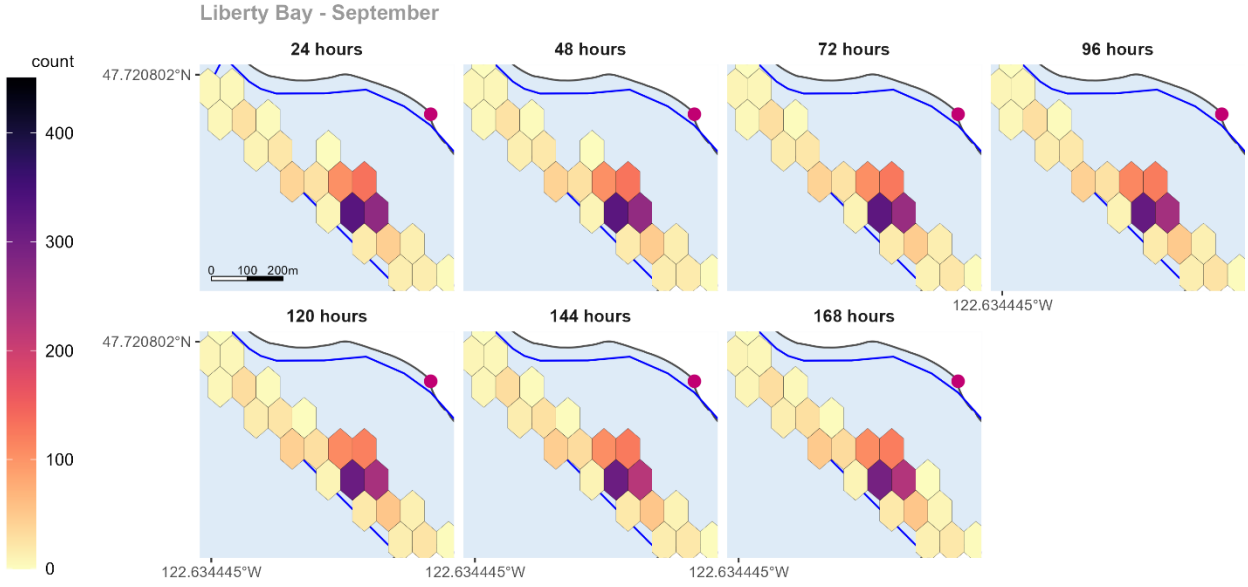

Figure 31. Simulated particle distributions in the Liberty Bay growing area for consecutive 24-hour time periods in September. The blue line shows the border of the approved growing area. Pink dots mark spill start points.

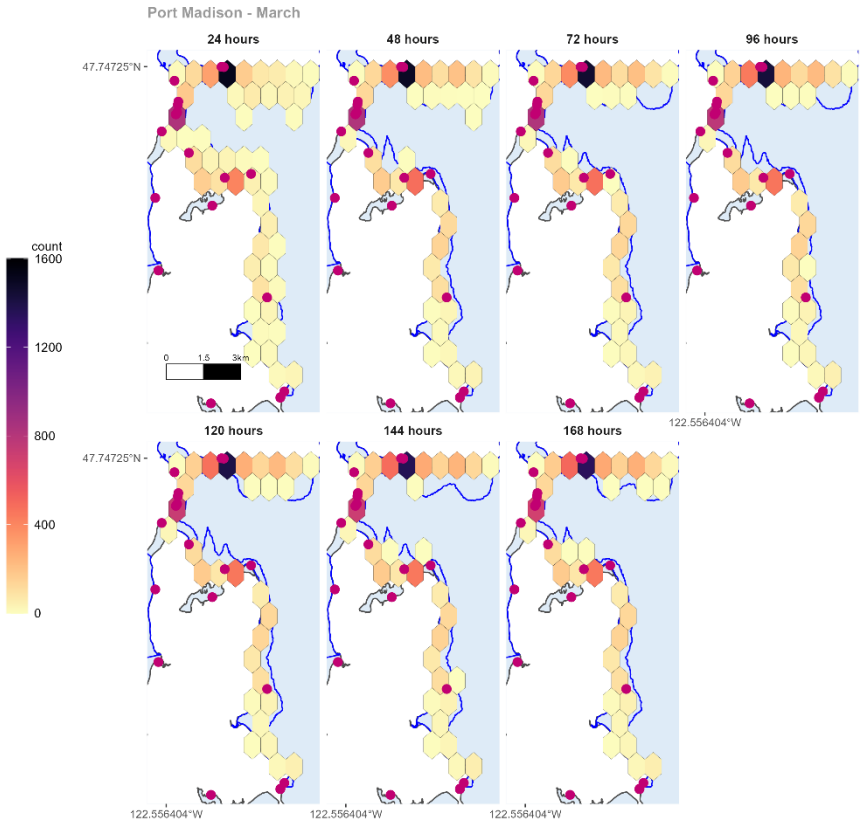

Figure 32. Simulated particle distributions in the Port Madison growing area for consecutive 24-hour time periods in March. The blue line shows the border of the approved growing area. Pink dots mark spill start points.

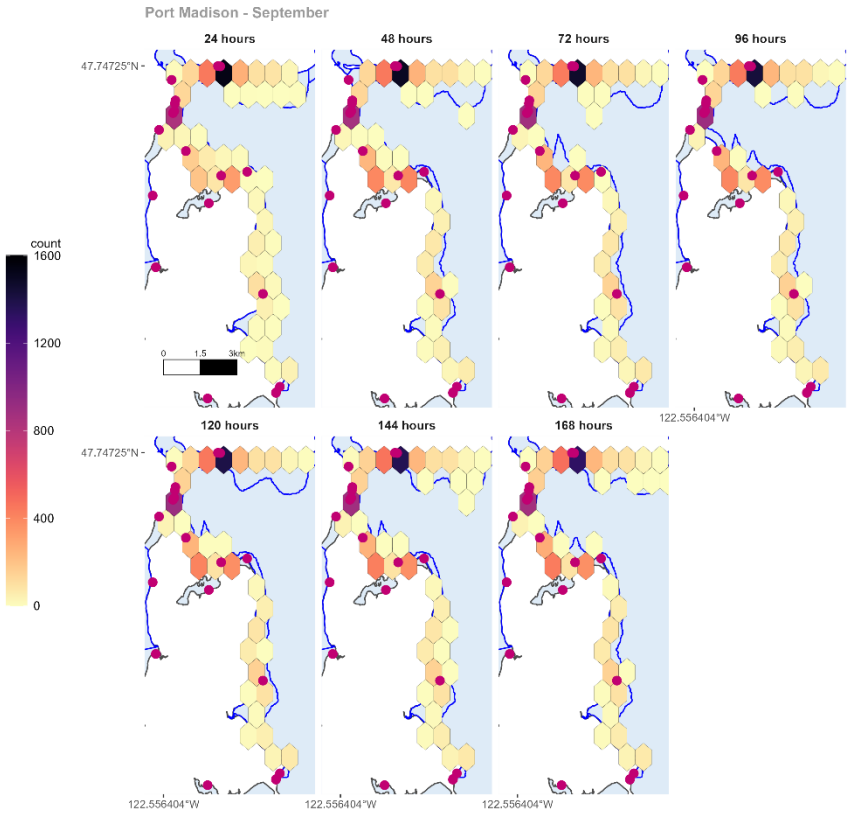

Figure 33. Simulated particle distributions in the Port Madison growing area for consecutive 24-hour time periods in September. The blue line shows the border of the approved growing area. Pink dots mark spill start points.

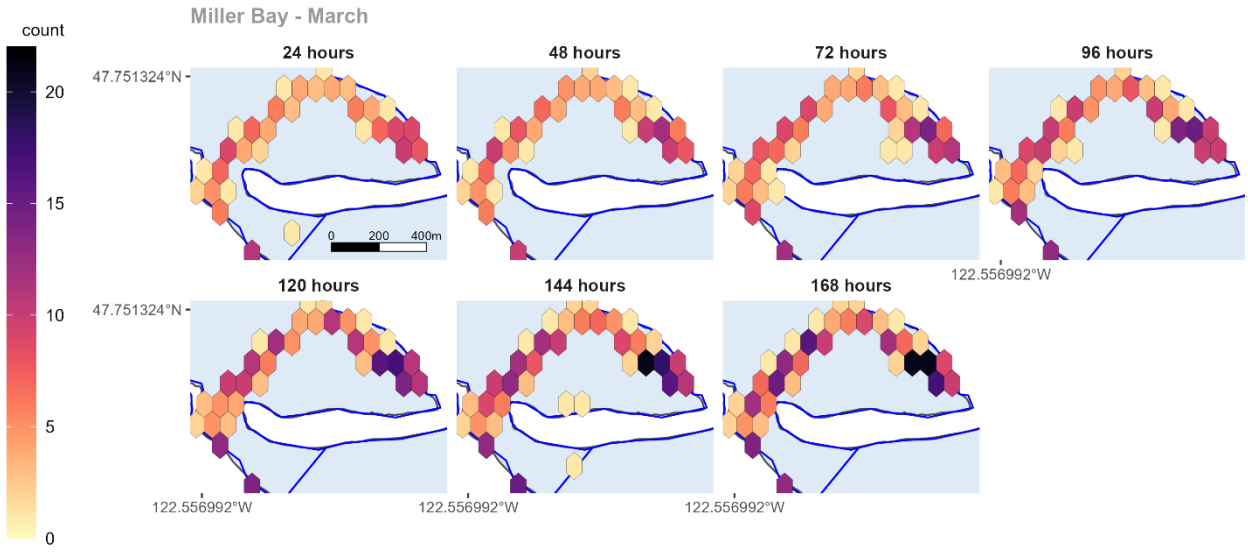

Figure 34. Simulated particle distributions in the Miller Bay growing area for consecutive 24-hour time periods in March. The blue line shows the border of the approved growing area.

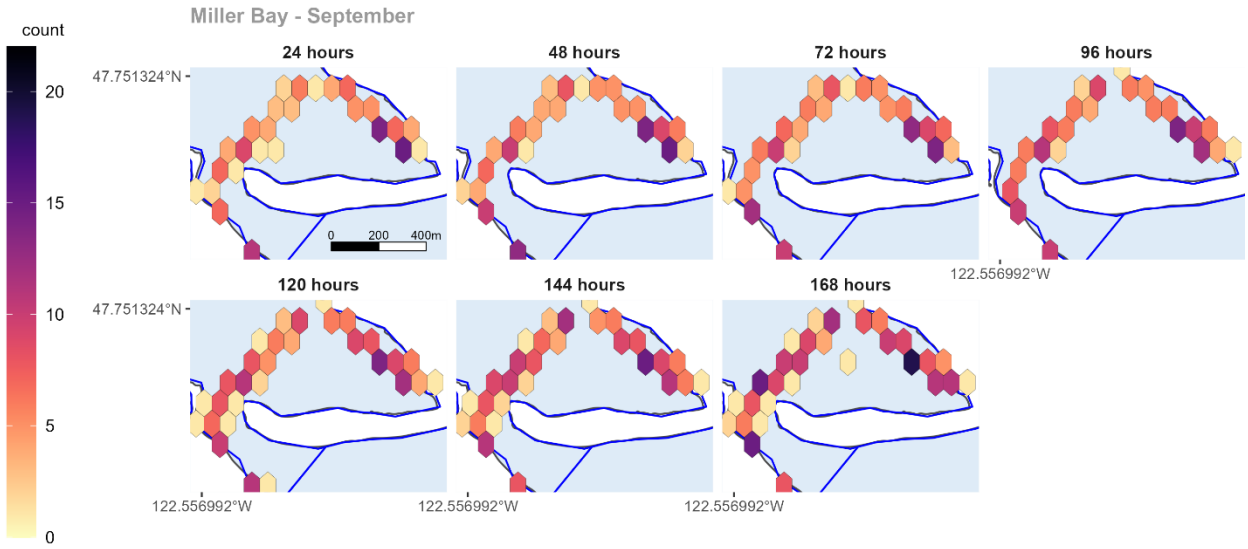

Figure 35. Simulated particle distributions in the Miller Bay growing area for consecutive 24-hour time periods in September. The blue line shows the border of the approved growing area.

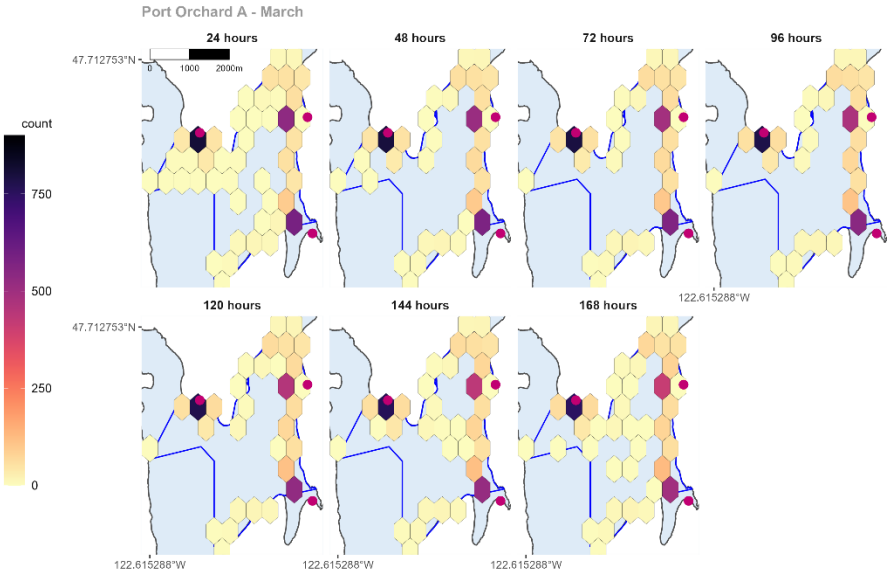

Figure 36. Simulated particle distributions in the Port Orchard A growing area for consecutive 24-hour time periods in March. The blue line shows the border of the approved growing area. Pink dots mark spill start points.

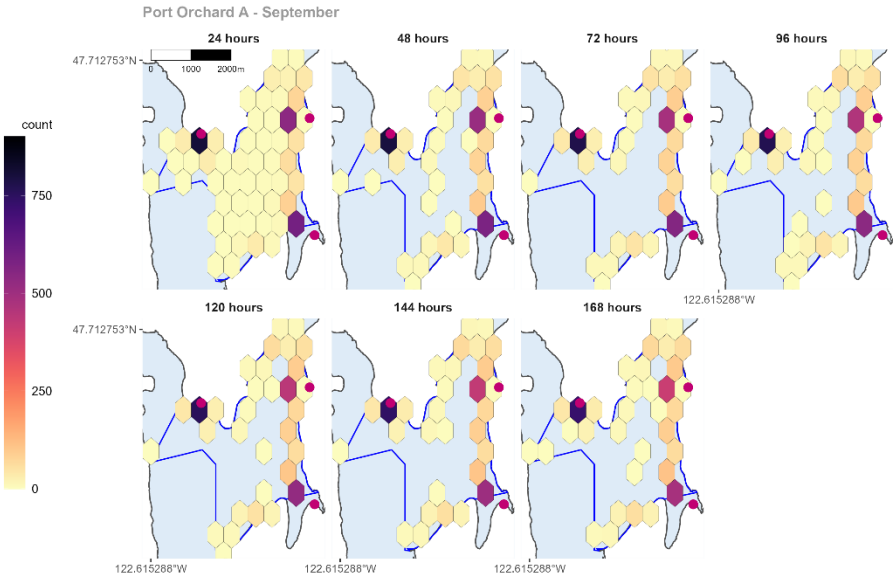

Figure 37. Simulated particle distributions in the Port Orchard A growing area for consecutive 24-hour time periods in September. The blue line shows the border of the approved growing area. Pink dots mark spill start points.

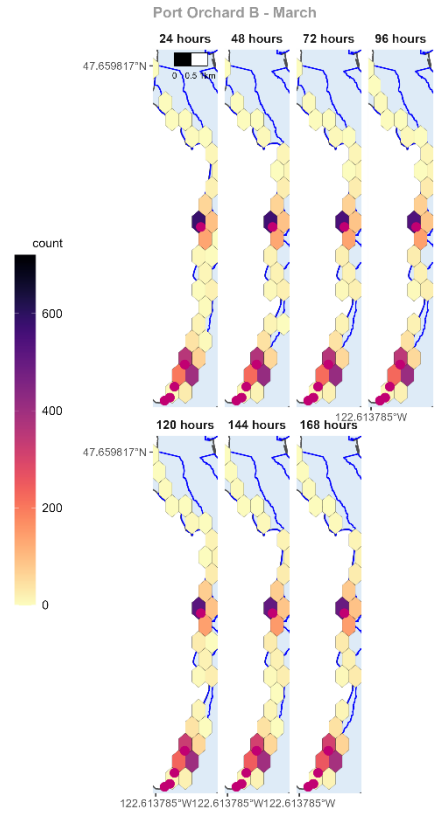

Figure 38. Simulated particle distributions in the Port Orchard B growing area for consecutive 24-hour time periods in March. The blue line shows the border of the approved growing area. Pink dots mark spill start points.

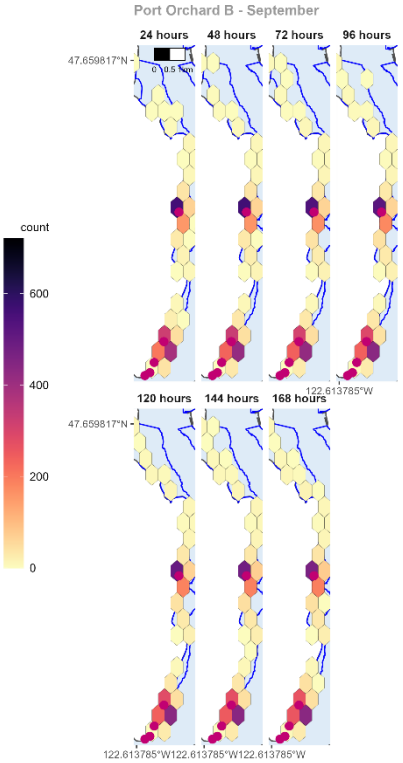

Figure 39. Simulated particle distributions in the Port Orchard B growing area for consecutive 24-hour time periods in September. The blue line shows the border of the approved growing area. Pink dots mark spill start points.

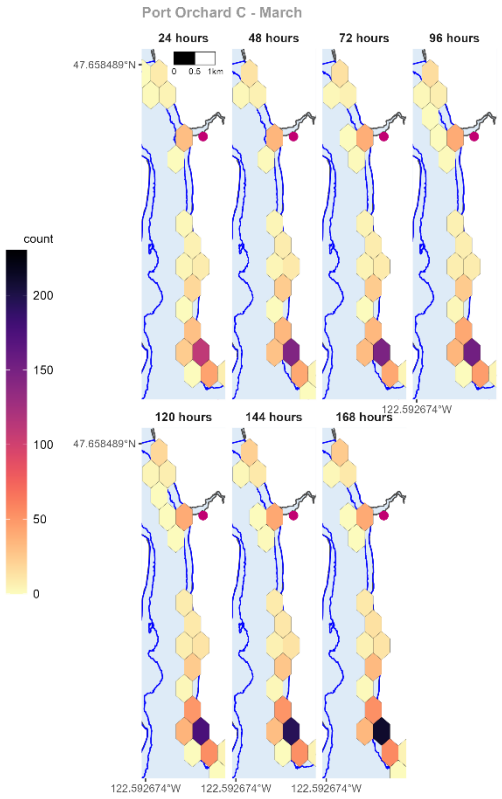

Figure 40. Simulated particle distributions in the Port Orchard C growing area for consecutive 24-hour time periods in March. The blue line shows the border of the approved growing area. Pink dots mark spill start points.

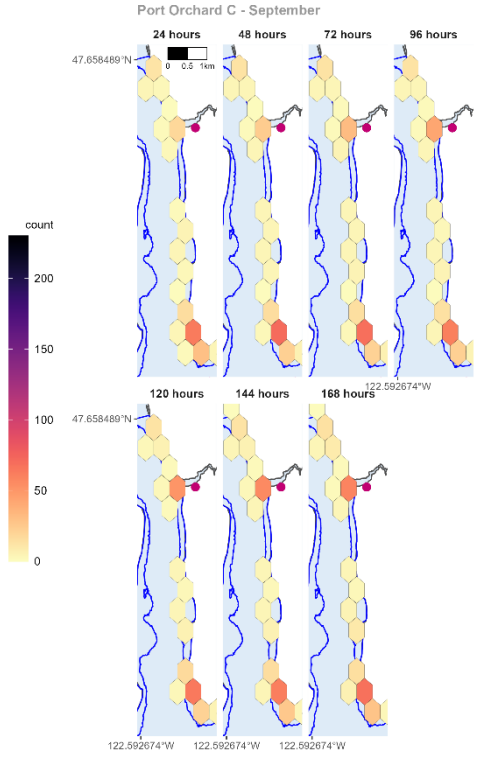

Figure 41. Simulated particle distributions in the Port Orchard C growing area for consecutive 24-hour time periods in September. The blue line shows the border of the approved growing area. Pink dots mark spill start points.

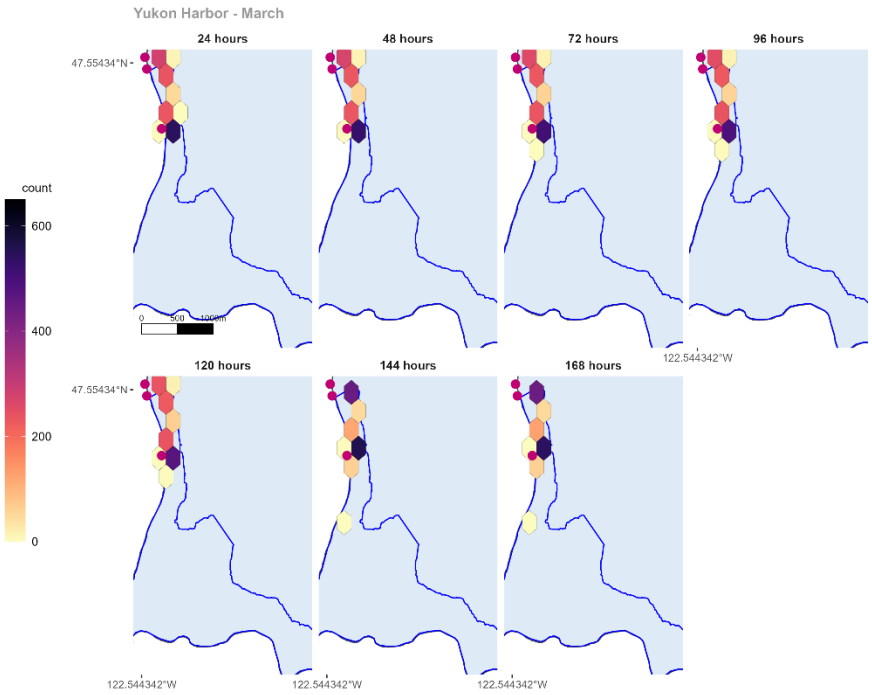

Figure 42. Simulated particle distributions in the Yukon Harbor growing area for consecutive 24-hour time periods in March. The blue line shows the border of the approved growing area. Pink dots mark spill start points.

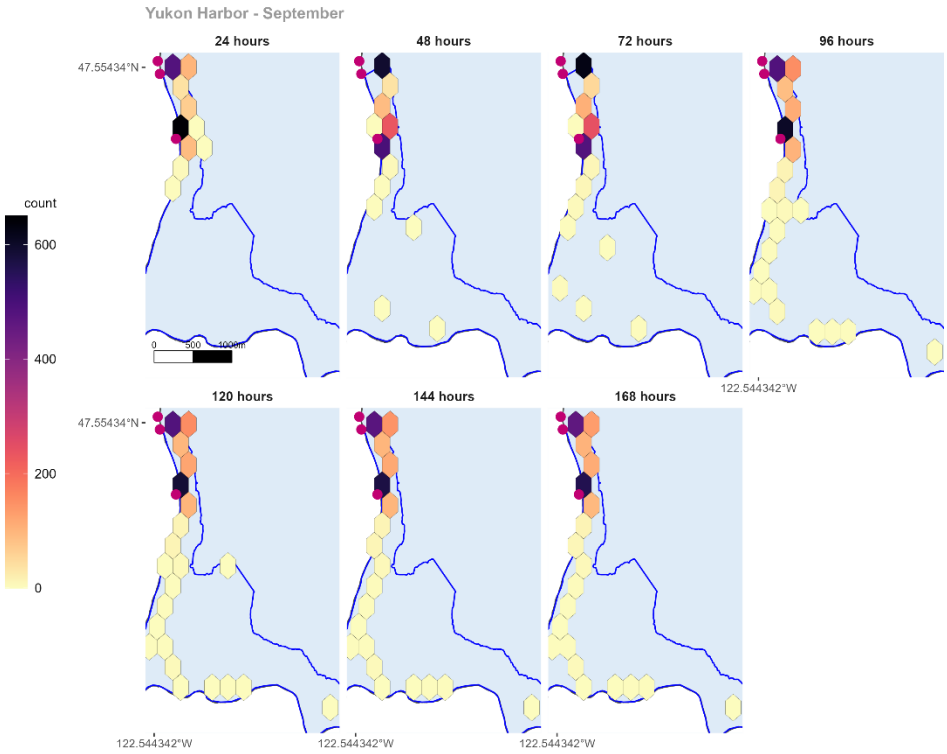

Figure 43. Simulated particle distributions in the Yukon Harbor growing area for consecutive 24-hour time periods in September. The blue line shows the border of the approved growing area. Pink dots mark spill start points.